AD-A195 182 CLUSTER BEAM STUDIES(U) HUGHES RESEARCH LABS MALIBU CA 1/1
W KNAUER ET AL. APR 88 AFOSR-TR-88-0544
F49620-85-C-0125

UNCLASSIFIED F/G 13/8 NL

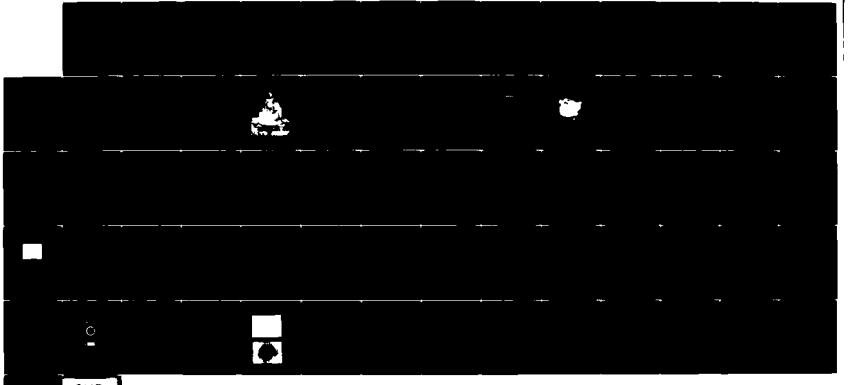

END
DATE FILMED
8 88

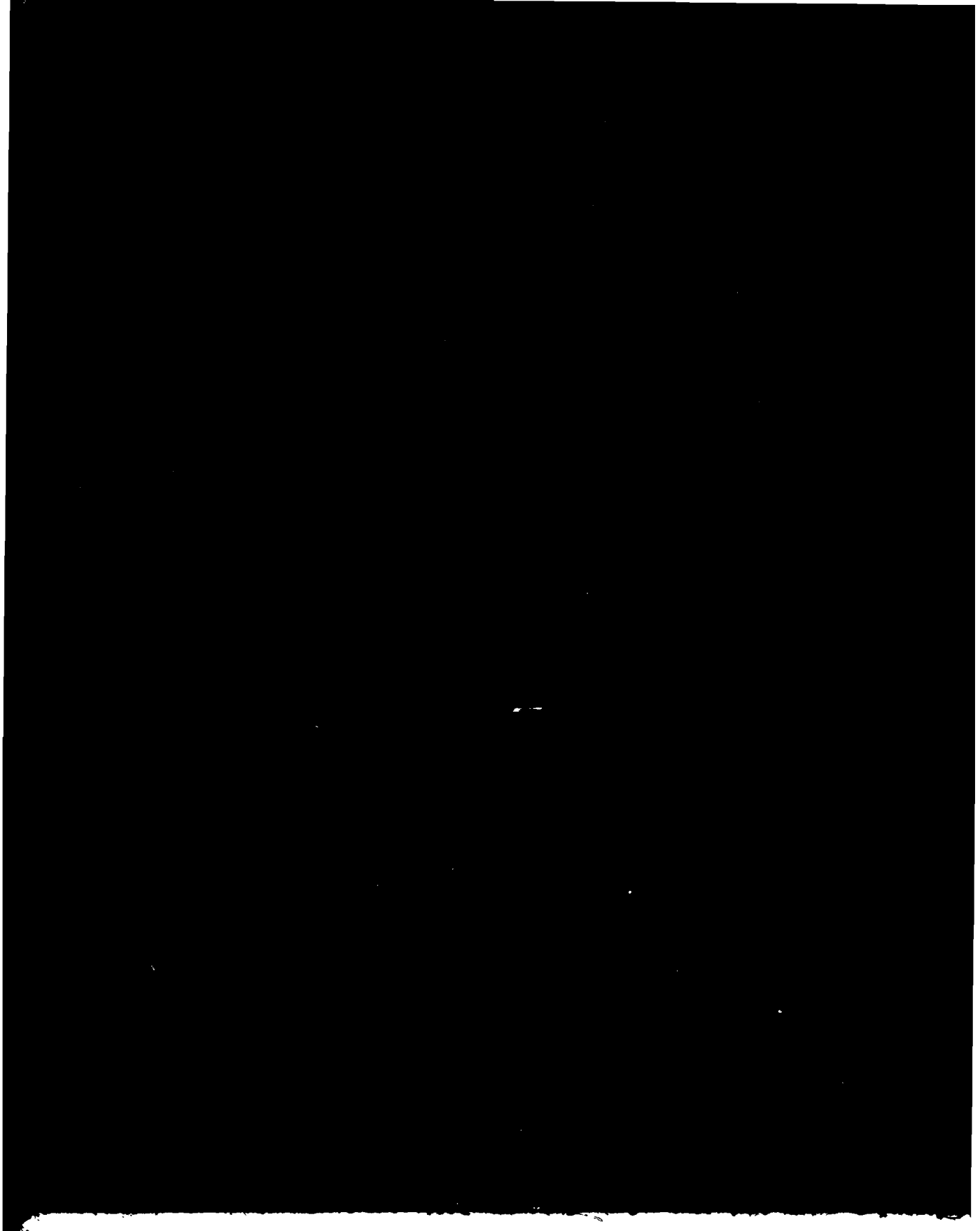

16669-2

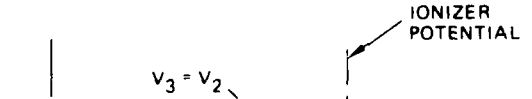

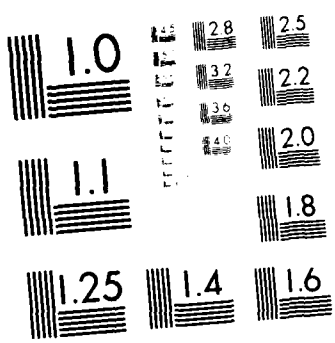

HAC Ref. F964

(2)

AD-A195 182

AFOSR-TR- 88-0544

CLUSTER BEAM STUDIES

W. Knauer and R.L. Poeschel

Hughes Research Laboratories
3011 Malibu Canyon Road
Malibu, California 90265

April 1988

F49620-85-C-0125

Final Technical Report
1 August 1985 through 31 October 1987

UNITED STATES AIR FORCE, AFSC
Air Force Office of Scientific Research
Bolling AFB, DC 20332-6448

UNCLASSIFIED
SECURITY CLASSIFICATION OF THIS PAGE

REPORT DOCUMENTATION PAGE

Form Approved OMB No. 0704-0188

1a. REPORT SECURITY CLASSIFICATION: Unclassified	1b. RESTRICTIVE MARKINGS
2a. SECURITY CLASSIFICATION AUTHORITY	3. DISTRIBUTION/AVAILABILITY OF REPORT: Unrestricted
2b. DECLASSIFICATION/DOWNGRADING SCHEDULE	
4. PERFORMING ORGANIZATION REPORT NUMBER(S)	5. MONITORING ORGANIZATION REPORT NUMBER(S): AFOSR-TR- 88-0544
6a. NAME OF PERFORMING ORGANIZATION: Hughes Research Laboratories; 6b. OFFICE SYMBOL (If applicable): HRL	7a. NAME OF MONITORING ORGANIZATION: Air Force Office of Scientific Research, Dir. of Electronic and Material Sciences
6c. ADDRESS (City, State, and ZIP Code): 3011 Malibu Canyon Road, Malibu, CA 90265	7b. ADDRESS (City, State, and ZIP Code): Building 410, Bolling AFB, DC 20332-6448
8a. NAME OF FUNDING/SPONSORING ORGANIZATION: Air Force Office of Scientific Research; 8b. OFFICE SYMBOL (If applicable): ~~AFSC~~ NE	9. PROCUREMENT INSTRUMENT IDENTIFICATION NUMBER: F49620-85-C-0125
8c. ADDRESS (City, State, and ZIP Code): Building 410, Bolling AFB, DC 20332-6448	10. SOURCE OF FUNDING NUMBERS: PROGRAM ELEMENT NO. 61102F; PROJECT NO. 2306/~~B2~~; TASK NO. B2; WORK UNIT ACCESSION NO.

11. TITLE (Include Security Classification): CLUSTER BEAM STUDIES (U)

12. PERSONAL AUTHOR(S): W. Knauer and R.L. Poeschel

13a. TYPE OF REPORT	13b. TIME COVERED	14. DATE OF REPORT (Year, Month, Day)	15. PAGE COUNT
Final	FROM 85/8/1 TO 87/10/31	1988, April	68

16. SUPPLEMENTARY NOTATION

17. COSATI CODES			18. SUBJECT TERMS (Continue on reverse if necessary and identify by block number)
FIELD	GROUP	SUB-GROUP	

19. ABSTRACT (Continue on reverse if necessary and identify by block number)

Cluster beams offer a means of depositing high-quality thin films at low substrate temperature for microelectronics fabrication. The advantage of cluster beam depositions is the ability to optimize the energy of the impacting particles, either directly in clustered vapors of nonvolatile materials or indirectly by bombarding the film during deposition with clusters of inert gases. When a cluster beam is ionized and accelerated through several thousand volts, clusters that contain 1000 or more atoms strike the surface with several electron volt energy per atom. The suprathermal energy of the depositing atoms is thought to produce unique thin films (either in quality, or in the ability to be deposited at all). This report describes the general effort on cluster beam formation methods, on cluster ionization by electron bombardment in a gridded ionization cell, on electrostatic mass-separation, and on electrostatic acceleration to a predetermined velocity. Detailed results are given on the improvements in performance of ionization cells for cluster beams of nonvolatile and gaseous materials.

20. DISTRIBUTION/AVAILABILITY OF ABSTRACT: ☐ UNCLASSIFIED/UNLIMITED ☒ SAME AS RPT ☐ DTIC USERS	21. ABSTRACT SECURITY CLASSIFICATION: Unclassified
22a. NAME OF RESPONSIBLE INDIVIDUAL: Mallory	22b. TELEPHONE (Include Area Code): 202-767-4939; 22c. OFFICE SYMBOL: NE

DD Form 1473, JUN 86 — Previous editions are obsolete.

SECURITY CLASSIFICATION OF THIS PAGE

UNCLASSIFIED

TABLE OF CONTENTS

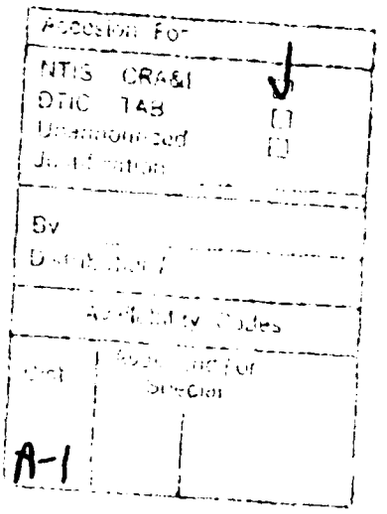

LIST OF ILLUSTRATIONS

LIST OF ILLUSTRATIONS (Continued)

SECTION 1

INTRODUCTION

This final report presents the results obtained under the Cluster Beam Studies Program performed for the Air Force by Hughes Research Laboratories under Contract F49620-85C-0125 DEF. The work was performed concurrently with cluster studies funded by Hughes Aircraft Company IR&D and under Navy Contract N00014-86C-0705. These efforts were closely coordinated, and results were shared to avoid duplication of effort. The objective of this Air Force program was to advance technology for ionization of clusters and for formation of ionized cluster beams that could be used in microcircuit fabrication. The technology developed was evaluated by film deposition. To place the Air Force Program in perspective, this report begins with a background section describing some selected elements of the Hughes overall cluster beam research program. The results obtained under this Air Force Program are described herein.

Cluster research was started at Hughes in 1983, with the objective of developing a low temperature film deposition process. The ionized cluster beam (ICB) technique described by Takagi at the University of Kyoto in Japan[1] was considered an excellent candidate for this purpose because it promised to provide control over the energy of the depositing atoms. According to Takagi, metal vapors could be clustered efficiently by expansion into vacuum through a nozzle. The resulting beam of neutral cluster atoms could then be ionized and accelerated electrostatically. Thereby, the directed energy with which the atoms struck the substrate could be controlled over a wide range. Because of the low charge-to-mass ratio of ionized clusters, a high flux of atoms with energies in the desirable 1 to 10 eV range could be achieved without space-charge limitation.

Initial work at Hughes sought to verify and improve the cluster formation process in crucible-type ICB sources, as described by Takagi. Because cluster ionization and beam formation was a serious concern in the development of crucible

ICB sources, this Air Force Program was proposed and awarded to address these problems. Before work began, however, Hughes investigation showed that the quantity of clusters obtained from crucible ICB sources was an insignificant fraction of the total vapor flux.[2]

Assuming that Takagi had indeed observed improvement in film quality under conditions of controlled, low-energy ICB deposition, it was reasoned that simultaneous impact of low-energy inert gas clusters during conventional vapor deposition could produce similar improvement. Hughes has called this approach "cluster-assisted deposition," under the supposition that impact of inert gas atoms with 1 to 10 eV energy will transfer energy to surface atoms in a depositing film, thereby improving film uniformity and increasing film density. Consequently, work under the Air Force Program concentrated on developing an improved ionization cell and acceleration system for using inert gas clusters to assist in deposition of metal vapors.

During the latter part of the program, we used the inert gas ICB system to evaluate cluster assisted deposition of metal films, with the emphasis on exploring deposition of gold on GaAs. This work made use of ionized inert gas clusters in the 500 to 2000 atom per cluster range to bombard the depositing film with atoms in the 2 to 5 eV per atom range. The films produced had good adherence and their appearance was excellent; however, they were not convincingly superior to vacuum-deposited films. Consequently, the value of inert-gas ICB-assistance in vapor deposition is not yet established. On the basis of our observations, we believe the film properties tend to show improvement as the ICB energy is increased. It is now considered probable that the improvements in film quality observed by Takagi's group were attributable to high energy atomic-ion bombardment, and not to the lower energy atoms of the clusters. If this is the case, the role of ionized cluster beams in film deposition remains to be determined, and the work reported here is only a first step.

SECTION 2

BACKGROUND

Ion cluster beam studies at Hughes Research Laboratories (HRL) include theoretical and experimental investigations of cluster formation, cluster ionization and acceleration, and cluster impact with surfaces. These research areas can be further divided into two categories: cluster formation from volatile or nonvolatile materials. Although the ionized cluster beam method was originated for direct deposition of nonvolatile materials, HRL research has shown that clusters of nonvolatile materials cannot be produced by crucible ICB sources in sufficient quantity to be practical for film deposition.[2,3] An alternative ICB technique using volatile materials (gases) has been conceived and, consequently, the discussion here is restricted to topics relevant to formation, ionization, acceleration, and application of inert-gas clusters.

Clusters are formed in volatile materials by isentropic expansion of gas at relatively high pressure through a supersonic nozzle into vacuum, as shown in Figure 1. A parametric study of this type of cluster formation has been reported by Hagena and Obert for the inert gases.[4] All the gas atoms and clusters in the central cone of the flow field are accelerated to the same velocity, and this velocity is a function only of the gas species and the nozzle temperature. The nozzle is fitted with a skimmer and an ionization cell, as shown in Figure 2, in order to obtain an ionized cluster beam. The clusters and gas atoms are ionized by electron bombardment in the ionization cell. Electrons emitted by the filament are accelerated across the gas stream by the potential applied to G1 and eventually collected on the anode grid G2. The drift velocity carries the ionized clusters and atoms to the extraction grid G3, where they are accelerated by the electric field resulting from the voltage applied between grids G3 and G4.

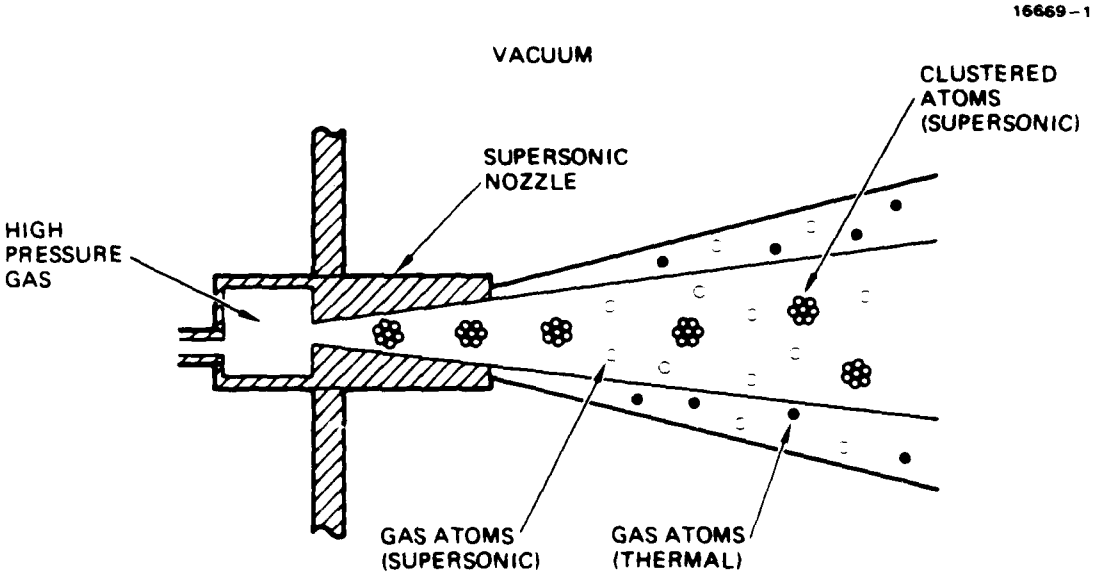

Figure 1. Illustration of cluster formation in gas expanded through a supersonic nozzle.

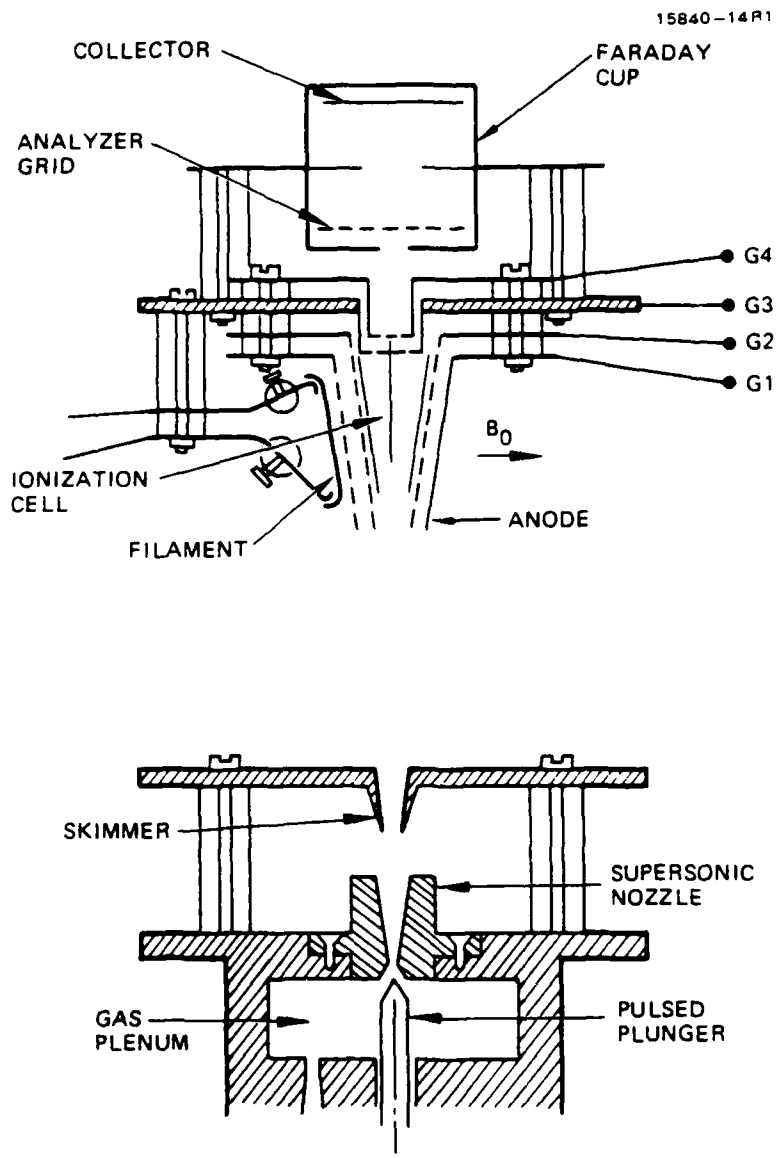

Figure 2. Ion cluster-beam experimental configuration.

Because the drift velocity v_s is the same for clusters and gas atoms in the core of the expansion, it is possible to determine the cluster size distribution using the voltage-current (i.e., retarding potential) characteristic measured with a gridded Faraday cup collector (see Figure 2). An idealized current-voltage characteristic is shown in Figure 3. The average cluster size N_a (in number of atoms per cluster) is defined by

$$N_a = \frac{2e\ (V_2 - V_1)}{m_o\ v_s^2} \quad , \tag{1}$$

where e is the electronic charge, V_1 is the anode voltage, V_2 is the voltage for which the collected ion current is one-half its maximum value, m_o is the atomic mass of the gas species, and v_s is the limiting velocity of the gas (as determined by the nozzle expansion parameters).

The ionized cluster beam has been predominantly characterized using the retarding potential measurement described above. Under ideal conditions, this method, and the voltage-current characteristic, can be used to determine the size distribution of ionized clusters. It should be noted, however, that the idealized voltage-current characteristic shown in Figure 3 is not always observed, especially when the ion beam is accelerated to high voltage. Thus, the average cluster size as defined above has been used to characterize cluster size unless the experiments performed were directed at investigating the implications of cluster size distribution. Also, the cluster size distribution in the extracted ion beam were intentionally altered in the experiments involving depositions. For ionized cluster beams for deposition or assisting deposition of thin films for microelectronic applications, atomic ions or small-cluster ions are thought to be undesirable in beams accelerated by high voltages, because they strike the substrate with substantial energy and can cause defects in the substrate or surface film.

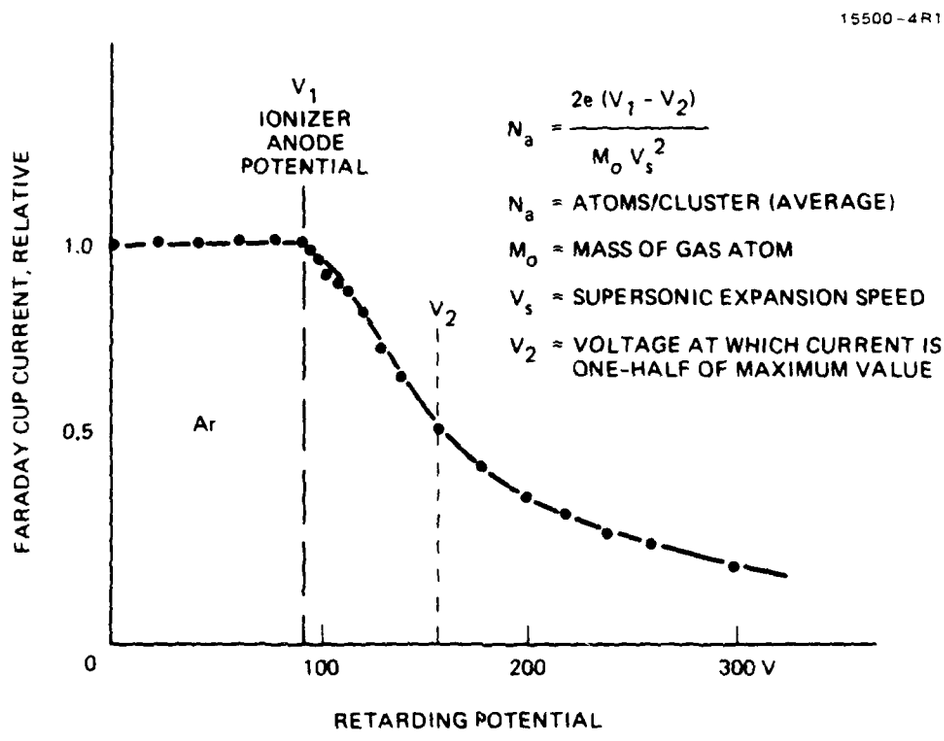

Figure 3. Representative data obtained in experiment to determine average cluster size, N_a.

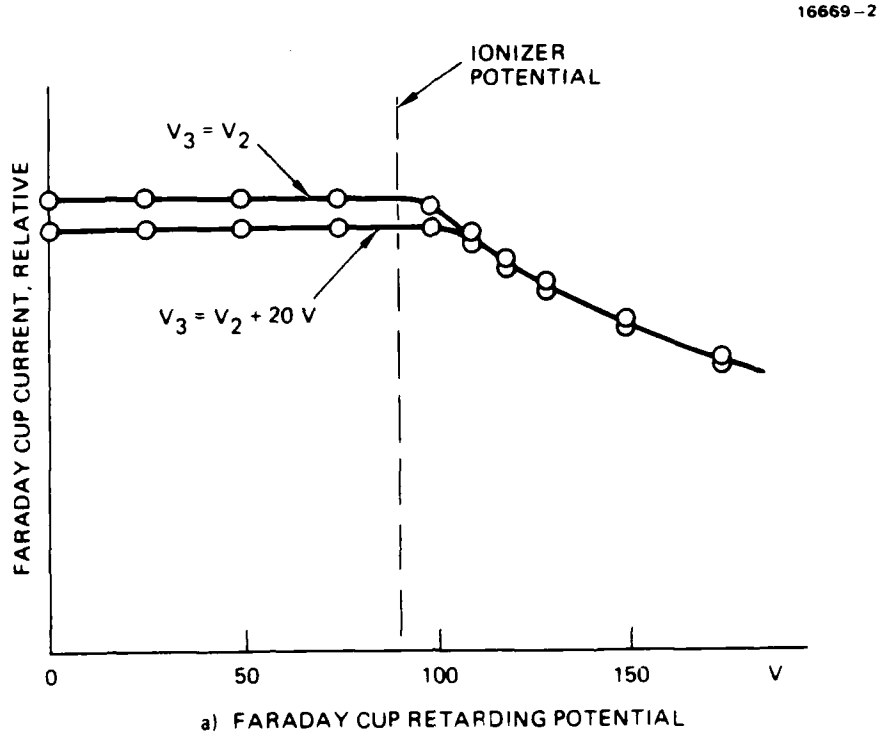

Figure 4. Measurements showing capability for achieving mass separation by biasing extraction grid relative to ionization-cell anode.

However, operating grid G3 at a higher voltage than the anode voltage (grid G2) can prevent atomic ions and small-cluster ions from entering the acceleration region. Figure 4(a) compares retarding potential characteristics obtained under conditions with and without mass separation bias. The resultant modification in cluster size distribution of the extracted ion beam is shown in Figure 4(b). It is apparent that the content of cluster ions in the extracted ion beam can be restricted to relatively large clusters if necessary.

In addition to determining the size of the ionized clusters in the extracted beam, it is of interest to know the total density of gas atoms in the ionization cell, and also the density and size distribution of neutral clusters. In the cluster study project at Hughes, neutral distribution has been measured with a directional pressure probe, and these measurements have been correlated with nozzle expansion relationships to permit calculation of the neutral atom density at any point in the nozzle exhaust as a function of the distance from the nozzle throat. Similarly, the size distribution and density of neutral clusters can be deduced from the size distribution and current density of ionized clusters by assuming appropriate ionization cross-sections. While this approach is not exact, it provides a useful estimate of the cluster formation and cluster ionization efficiencies.

An alternative ICB technique was invented to assess the benefit of the ICB technique in film deposition, whereby inert gas cluster ions could transfer energy to the growing film and increase the mobility of the surface atoms. Figure 5 is a schematic diagram of the cluster-assisted film deposition system. The cluster source is operated in bursts of 1 to 2 μs duration at repetition rates up to 10 Hz. For most of the experiments performed, vapor source and cluster source were operated so that the time-averaged atomic flux impacting the substrate was approximately the same for both metal vapor and ICB sources. It

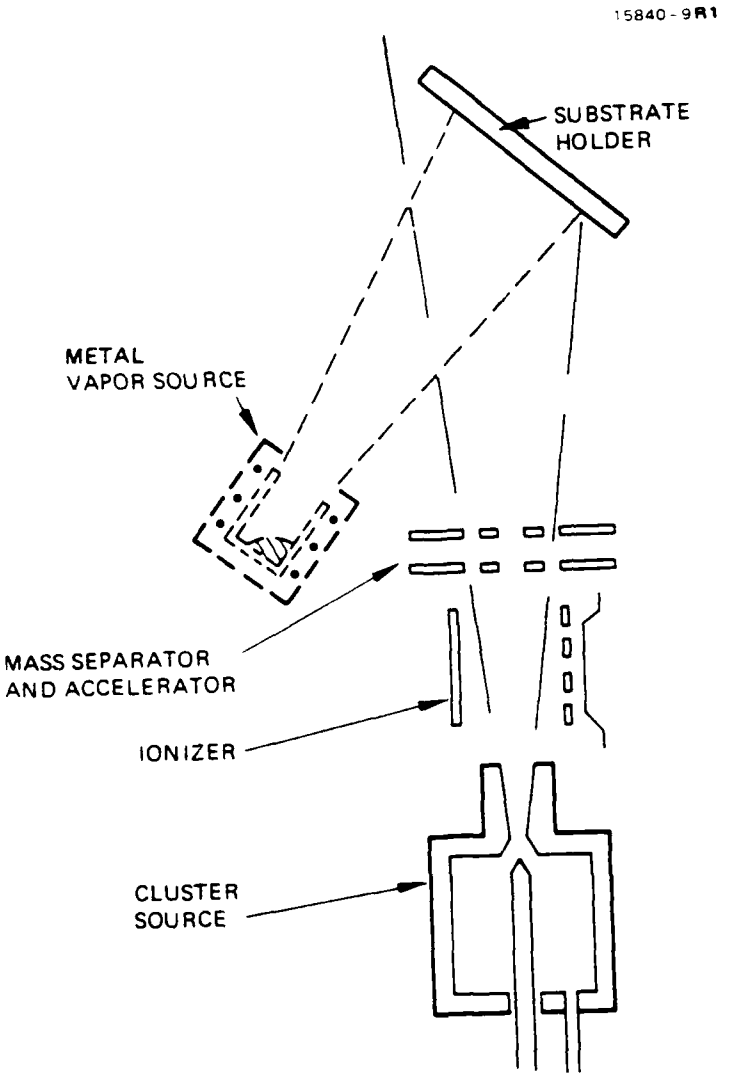

Figure 5. Cluster-assisted film deposition system, incorporating a pulsed noble gas cluster source and a conventional crucible-type metal vapor source.

has been assumed that the ionized clusters decompose into atoms upon impact, and that the cluster energy is divided equally among atoms. Neither of these assumptions has been verified at this time. The substrate holder has provisions for heating the substrate; however, the angle of incidence for the ICB and metal vapor are fixed as shown (the axis of the ICB source makes an angle of 30° with the normal to the substrate). Figure 6 is a photograph of the apparatus.

MC16747

17441-1

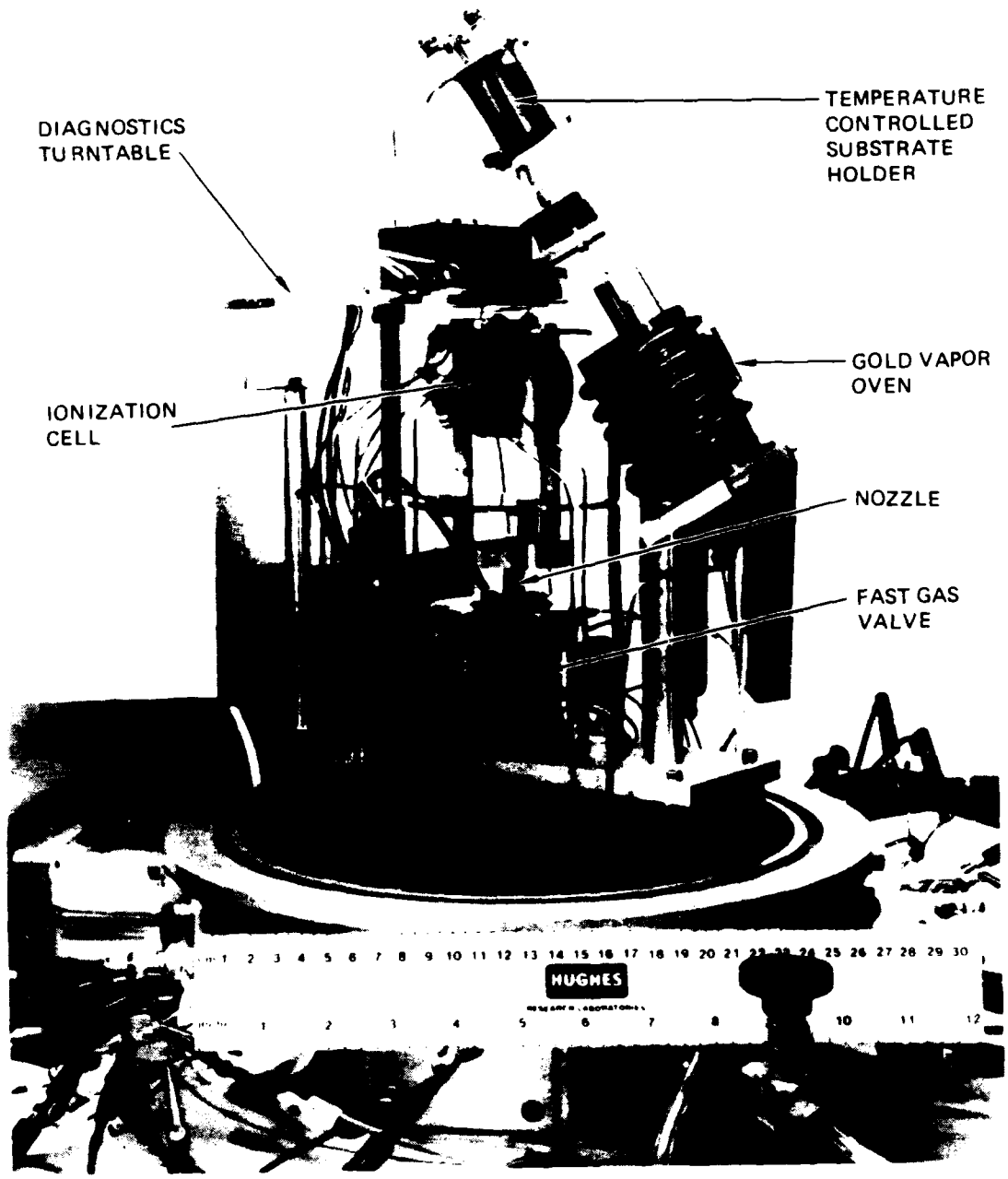

Figure 6. Facility for inert-gas cluster-assisted deposition of metal vapor.

SECTION 3

ACCOMPLISHMENTS

Much of the work completed under this program was reported in the Annual Report for 1985-86. The studies of ionization technology for nonvolatile clusters were discontinued when it was concluded that cluster formation was too inefficient for practical film deposition, and consequently description of that work is not repeated here.

3.1 CLUSTER FORMATION AND IONIZATION

Work under this program began with analyses of the results obtained previously with a variety of nozzle and ionization cell configurations. For gases, reliable cluster formation had been achieved using conical nozzles with 8° apex angle, 0.5 mm throat diameter, and expansion ratios of about 100. Operated in the configuration shown earlier in Figure 2, these nozzles produced relatively large clusters using argon (2000 to 5000 atoms per cluster) with a relatively low reservoir pressure (2 to 3 atmospheres absolute). In this early operating mode, the gas input to the vacuum system was relatively high, and it was necessary to limit the pulse repetition rate to 1 Hz or less to maintain the ambient pressure in the 10^{-4} Torr range. Because the objective of volatile cluster studies under this program was to develop an ionized cluster beam system for demonstrating the validity of cluster-assisted film deposition, we were interested in the following, somewhat different cluster parameters:

- ICB diameter of 1.5 cm
- ICB current density of 10 $\mu A/cm^2$
- Nominal cluster size of 2000 atoms per cluster

- Cluster energy of 1 to 2 eV/atom (2000 to 4000 V accelerating voltage)
- Duty cycle of at least 10% (10 Hz repetition rate).

Obviously, it was necessary to reduce the gas throughput, reduce the cluster size, and increase the repetition rate (i.e., the duty cycle) without loss of cluster production efficiency. To achieve these improvements, we started scaling the nozzle dimensions in accordance with the guidelines described by Hagena and Obert.[4] The nozzle throat diameter was decreased to 0.25 mm to reduce the gas throughput, and the expansion ratio was increased to about 156 to produce 2000 atom-clusters at the desired reservoir pressure of 3000 Torr. An attempt to further reduce the throat diameter to 0.127 mm, using a high expansion ratio (1300) nozzle, produced anomalous results when compared with the results reported by Hagena and Obert (as shown in Figure 7), and we elected to work with the larger throat diameter (0.254 mm). This nozzle is operable at 10 Hz with 2 μs pulse length using argon gas at acceptable ambient pressure.

3.1.1 Ionization Chamber Geometry and Operating Characteristics

Having achieved acceptable gas flow conditions, we concentrated on refining the ionization cell configuration and defining the operating conditions to produce useful ionization efficiency under formation of the ionized cluster beam. Figure 8 illustrates the configuration developed, and Figure 9 is a photograph of the ionization cell hardware. A detailed account of the development iterations would serve no real purpose; however, it is appropriate to point out some essential features of the cluster source and beam forming system. First, it is very important that the ionization cell be located at a sufficient distance from the nozzle to permit "skimming" of the gas that is not clustered and, thereby, keep a low concentration of atomic gas in the ionization cell. Similarly, it is important that the

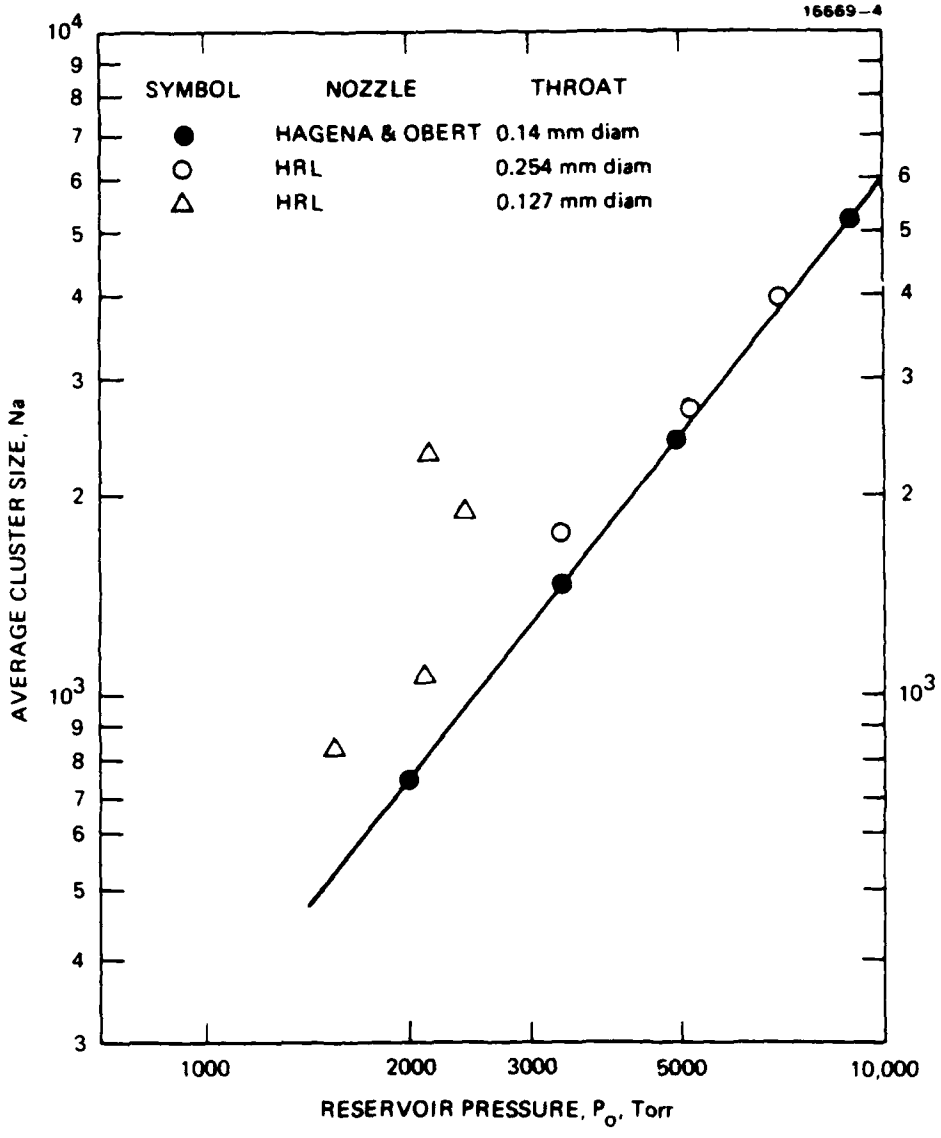

Figure 7. Comparison of results for experimental determination of average cluster size versus reservoir pressure. Nozzle scaling relationship of Hagena and Obert[2] used to adjust pressure.

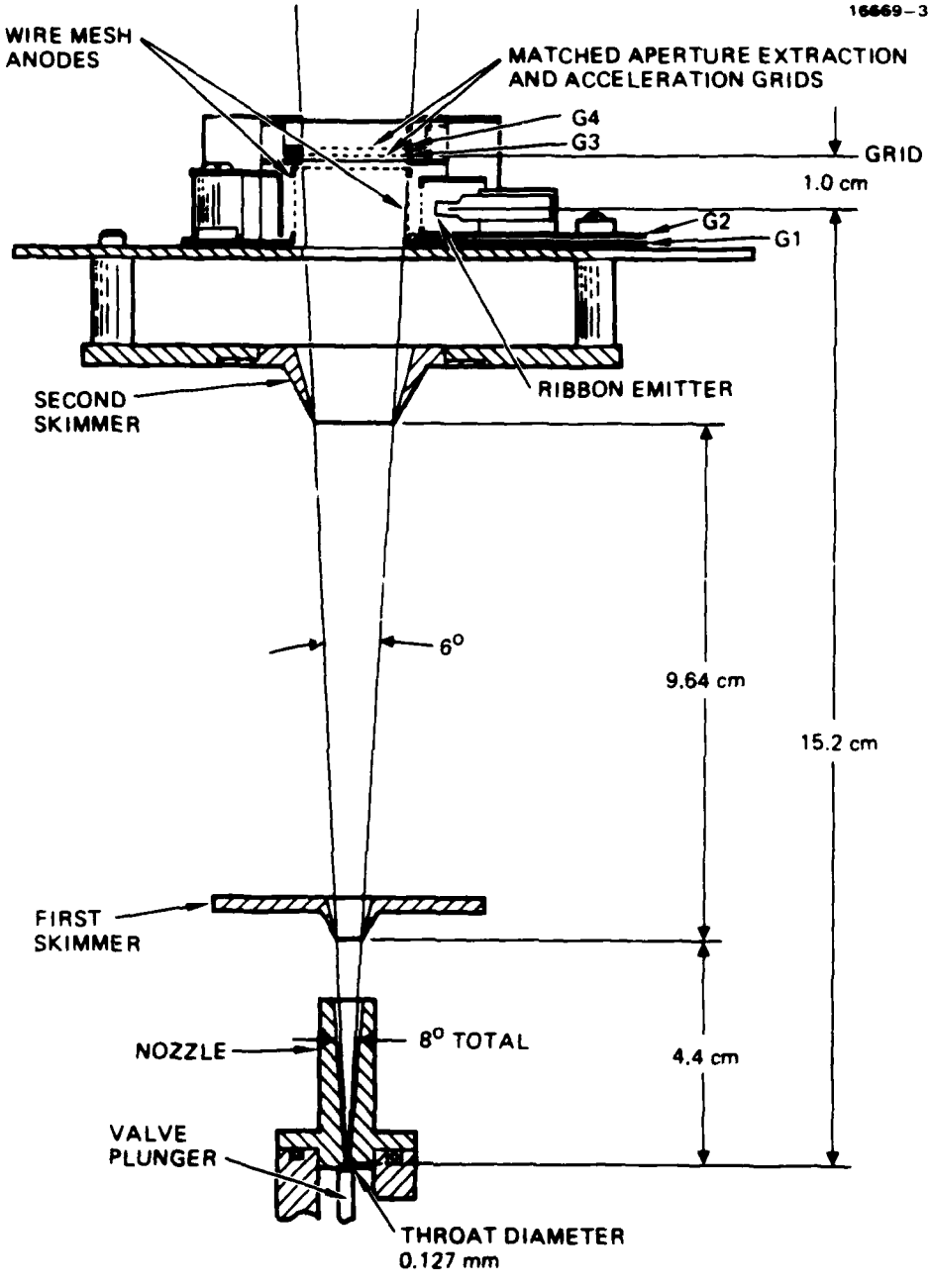

Figure 8. Experimental configuration for second iteration on ion cluster source.

M16748

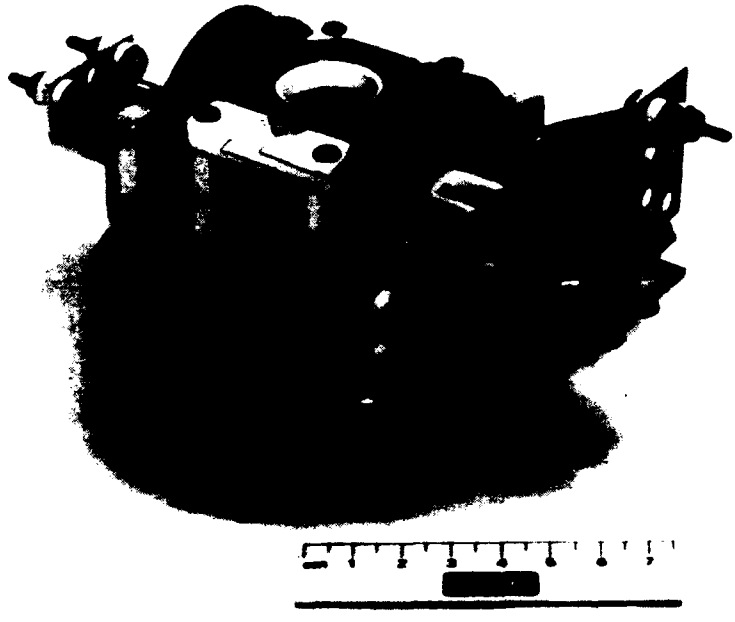

Figure 9. Photograph of the ionization cell that is shown schematically in Figure 8.

ionization cell structure be kept very "open" so that gas is not trapped in the cell (which would increase the ambient density and result in destruction of clusters in the ionization cell). The volume of the ionization cell traversed by the ionizing electrons must be kept suitably small. We found that it was undesirable to attempt to severely limit this volume using a magnetic field aligned with the ionizing electron stream. Consequently, the coils visible in the photograph of Figure 9 were only used initially and were eventually removed. A large plasma region resulted in multiple ionization of clusters and extraneous discharges that impaired application of acceleration voltage.

3.1.2 The Cluster Ionization Process

Except for one early paper,[5] very little attention has been given, so far, to the basic processes associated with cluster ionization. Yet, many issues of practical importance and of basic interest have arisen. Below, we will address such questions as: How does the ionization probability vary with cluster size, How important are multiple ionizations, and How completely can a cluster beam be ionized?

At first, we will briefly consider the two types of possible interactions between bombarding electrons and clusters. In metal clusters (larger than a few hundred atoms), the valence electrons are free, as in bulk metals, and ionization is expected to occur when one of these free electrons is scattered out of the cluster by an impacting electron. Qualitatively, this ionization process is identical to secondary electron emission from bulk metal surfaces. Quantitatively, however, the process is expected to involve modified ejection probabilities because of the small dimensions of clusters.

A different situation arises in gaseous (volatile) clusters. Here, cluster atoms are attached to each other by dispersion (van der Waals) forces, and valence electrons remain attached to the

individual atoms. Accordingly, bombarding electrons must ionize individual atoms, and the released electrons must drift to and eject from the cluster surface, if a cluster is to be ionized.

As far as empirical ionization cross-sections are concerned, no data exist for either cluster type. In fact, such data may not be easy to provide, because clusters can carry more than one charge (see below). To determine such higher charge levels, one needs to measure not only e/m, but also cluster mass m, which, itself, has so far been elusive.

In this situation, cluster ionization cross-sections can be obtained only through theoretical estimates. Because recent work at HRL has tended toward the use of volatile clusters, we have primarily sought to estimate ionization cross-sections of van der Waals type clusters. A brief summary of this effort follows.

In general, when a bombarding electron strikes a cluster, it penetrates into the interior, causing ionizations and excitations as it advances (see Figure 10). The number of ions generated thereby is determined by the product of the number of atoms k that an electron moves past, and the atomic ionization probability P. The former quantity is given by

$$k = \left(\frac{4}{3}\right)^{2/3} \left(\frac{i}{\pi}\right)^{1/3} ,$$

where i is the number of atoms in the cluster. The latter quantity is simply the ratio of ionization cross-section q to atomic cross-section a^2:

$$P = q/a^2 .$$

Accordingly, the number of ionizations becomes

$$\bar{z} = \left(\frac{4}{3}\right)^{2/3} \left(\frac{i}{\pi}\right)^{1/3} \frac{q}{a^2} .$$

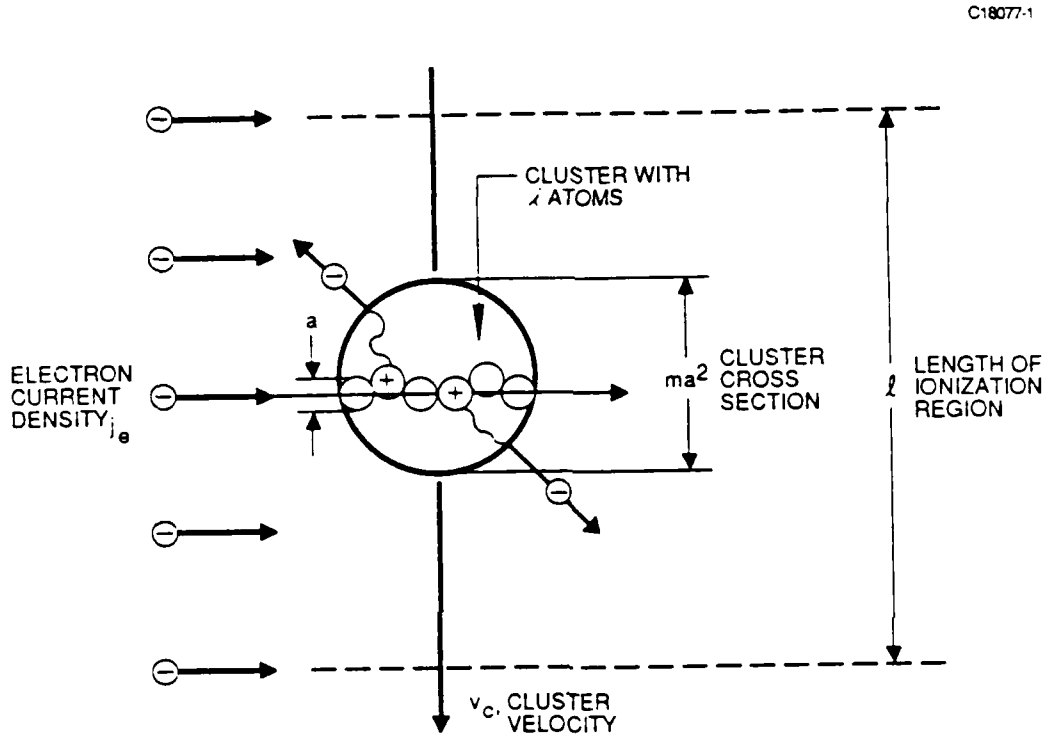

Figure 10. Volatile cluster ionization process: electrons passing through a cluster, randomly ionize individual atoms. In order that the cluster becomes ionized, the released orbital electrons must drift to the cluster surface and eject into vacuum.

We have evaluated this expression for clusters with 1000 atoms under bombardment with 100 eV electrons (where the ionization rate is near a maximum). Table I shows that, for most gases (with the exception of helium), clusters tend to become multiply ionized under these conditions. Actually, the above derived ionization number $\bar{z}$ is an average value. Among the numerous clusters struck by electrons, the value N_i will fluctuate statistically. If these fluctuations follow Poissons law, the probability of a cluster becoming ionized z = 0, 1, 2, 3.... times by a single electron is

$$P_k(z) = (\bar{z})^z \cdot N_i \frac{1}{z!} \exp(-\bar{z}) \quad .$$

To assess the magnitude of this spread in z, we consider the case of argon clusters with 1000 atoms, bombarded by electrons with 100 eV. According to Table I, the average number of ionizations N_i expected in this case is 2. The above derived expression, however, predicts probabilities of 0.15, 0.28, 0.27, and 0.17 for clusters attaining 0, 1, 2, and 3 charges, respectively. Accordingly, the number of charges varies widely from cluster to cluster.

So far, only ionizations produced by a single electron have been considered. To determine the overall ionization probability for a cluster, one must add up, statistically, ionizations by electrons that pass through a cluster at all possible surface elements, each with area a^2. The number of such elements is

$$m = \left(\frac{3}{4\pi}\right)^{2/3} {}_i^{2/3} \quad .$$

The probability of an electron passing through one of these elements is determined by the intensity of the electron bombardment (current density j_e), by the dwell time t of the

TABLE I. Cluster Ionization Probabilities (for 1000 Atom Clusters).

Gas	Ionization Cross-section for 100 eV Electrons	Ionization Probability Per Cluster Atom	Number of Ions Generated Per Electron
He	4×10^{-17}	0.028	0.23
Ar	3.5×10^{-16}	0.24	2.0
Xe	7×10^{-16}	0.3	3.0
N_2	3×10^{-16}	0.41	3.4
O_2	3×10^{-16}	0.31	2.6
CO_2	3×10^{-16}	0.19	1.6

cluster in the electron stream, and by the area a^2 of the element. If the dwell time t is expressed in terms of the length of the ionization region, ℓ, and of the cluster velocity, v_c, the number of electrons passing through an element a^2 becomes

$$\bar{y} = \frac{j_e \ \ell a^2}{e \quad v_c} \quad .$$

Furthermore, the number of electrons passing through an entire cluster with m elements is

$$\bar{Y} = m\bar{y} \quad .$$

Because many electrons pass through many clusters, significant fluctuations in the numbers of passages can be expected. For a Poisson distribution, the probabilities of Y = 0, 1, 2, 3.... electron passages are given by

$$P_m(Y) = (\bar{Y})^Y \ \frac{1}{y!} \ \exp(-\bar{Y})$$

Finally, the probabilities of Z = 0, 1, 2, 3.... ionizations of an entire cluster follow from

$$P_{m,k}(Z) = \Sigma P_m(Y) \ P_k(z) \quad .$$

Here, $P_{m,k}$ consists of a sum of terms, because each level of ionization Z can be reached with various combinations of numbers of ionizations z per electron, and numbers of penetrating electrons Y. We have numerically evaluated this expression for argon clusters bombarded with 100 eV electrons. Figure 11 shows the resulting ionization probabilities for singly-, doubly-, and triply-charged clusters.

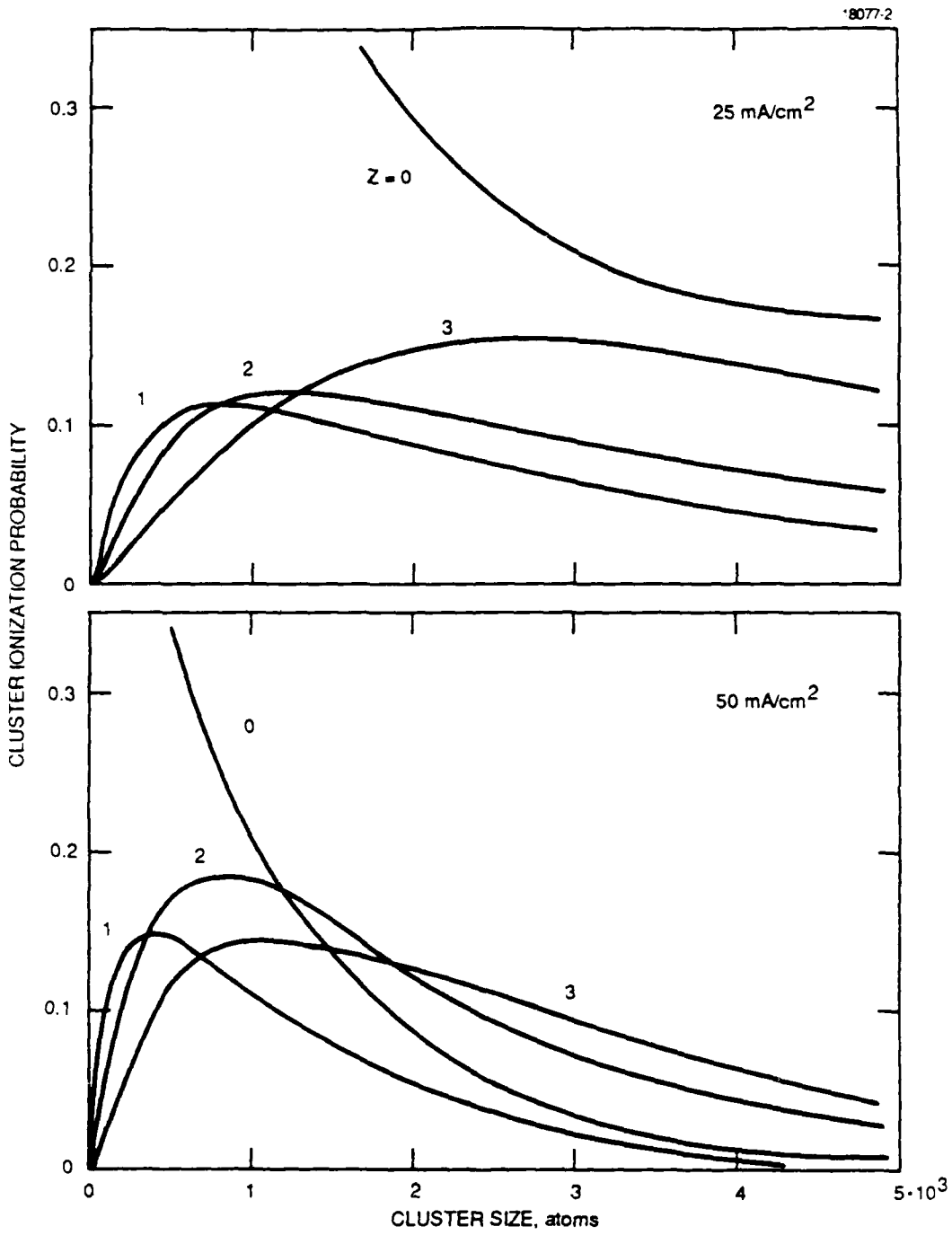

Figure 11. Theoretically determined cluster ionization probabilities for argon clusters, bombarded with 100 eV electrons. The clusters are assumed to move at speeds of $v_c = 3 \cdot 10^4$ cm/sec through a drift length l=1 cm being exposed to electron currents of 25 and 50 mA/cm^2. The parameter Z is the charge level.

We can draw a number of conclusions from the results shown in Figure 11. First, under the operating conditions typically used at HRL (clusters with thousands of atoms, ionization currents of 10 to 100 mA, ionization energies of 50 to 100 eV), most clusters can be expected to become ionized (note: curves for Z=0 are for the probability of a cluster remaining neutral). Measurements of the cluster current as a function of ionizing current confirm this, by indicating a saturation level for ionized clusters in the range of 30 to 40 mA/cm^2 (see Figure 12).

Second, very significant numbers of clusters become multiply charged, which suggests that clusters are substantially larger than previously thought. We estimate that a cluster beam that, according to earlier methods of assessments, had an average cluster size of 1000 atoms, actually should average about twice this size. It is noteworthy that this result does not imply changes in the total atom flux contained in ionized clusters, nor in the energy per atom in an accelerated cluster beam. In fact, both quantities remain exactly the same. This conclusion follows from the fact that the measured mass-to-charge ratio remains unchanged. The larger-than-expected size of clusters has one favorable consequence: it permits the transmission of large cluster fluxes with less space-charge spreading.

3.1.3 Cold Cathode Cluster Ionization

Cluster ionization cells require electron sources that can provide 10 to 100 mA of electrons. For noble gas and metal cluster beams, thermionic electron sources have proved to be convenient and reliable. For reactive gases, such as chlorine and oxygen, which now are considered for cluster applications at Hughes, thermionic sources are unsuitable because they deteriorate rapidly. A major factor thereby is the elevated temperature that accelerates reactions between cathode surface and reactive gas. Accordingly, cold cathodes would be preferable. To obtain electron emission from a cold metal

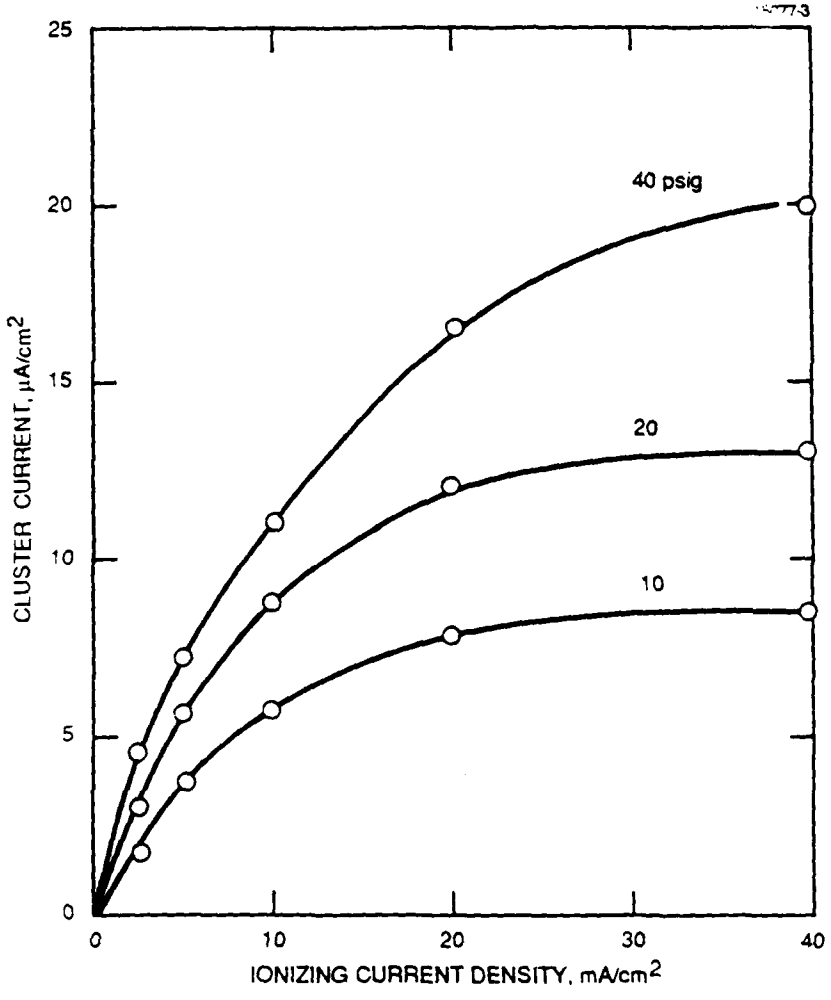

Figure 12. Argon cluster current density, measured as a function of bombarding electron current density (electron energy 100 eV, length of the ionizing region 2 cm). The bending over of the curves is interpreted as the beginning of full ionization.

requires either photon or energetic particle bombardment. In cold cathode glow discharges, for example, energetic ions, which bombard the cathode, can provide efficient emission of electrons. Such glow discharges require gas pressures on the order of Torrs. In cluster beams generated by supersonic expansion, pressures of this magnitude exist directly in front of the mouth of the expansion nozzle.

We have explored cluster ionization with electrons from a cold cathode discharge adjacent to the expansion nozzle. By surrounding the nozzle exhaust with a cylinder [see Figure 13(a)] and by applying a voltage in excess of 500 V between cylinder (cathode) and nozzle (anode), we were able to maintain a stable glow discharge inside the cylinder. We believe that this discharge consists of a positive column within the boundaries of the supersonic beam, and a cathode fall between beam edge and cathode electrode [see Figure 13(b)]. Atomic ions from the positive column are accelerated across the cathode fall to strike the cathode, where they release secondary electrons. To confirm this model, we have compared the ionized cluster energy distribution of this ionizer with that from two other ionizers. One of these reference ionizers also had a cold cathode, and, in addition, was equipped with an anode grid [see Figure 13(b)]. This grid was added to tie the positive column to anode potential. The other reference ionizer was a thermionic configuration [see Figure 13(c)]. Cluster energy distribution curves, obtained with all three configurations, are shown in Figure 14. The nearly identical cold cathode distributions indicate that, even without anode grid, cluster ionization occurs within a narrow range of the anode potential level, confirming that the positive column readily adopts anode (=nozzle) potential. Furthermore, the similarity with the thermionic ionizer curve (obtained with a beam acceleration voltage of 600 instead of 500 V for the two cold cathode configurations, but with the same supersonic beam conditions) gives additional

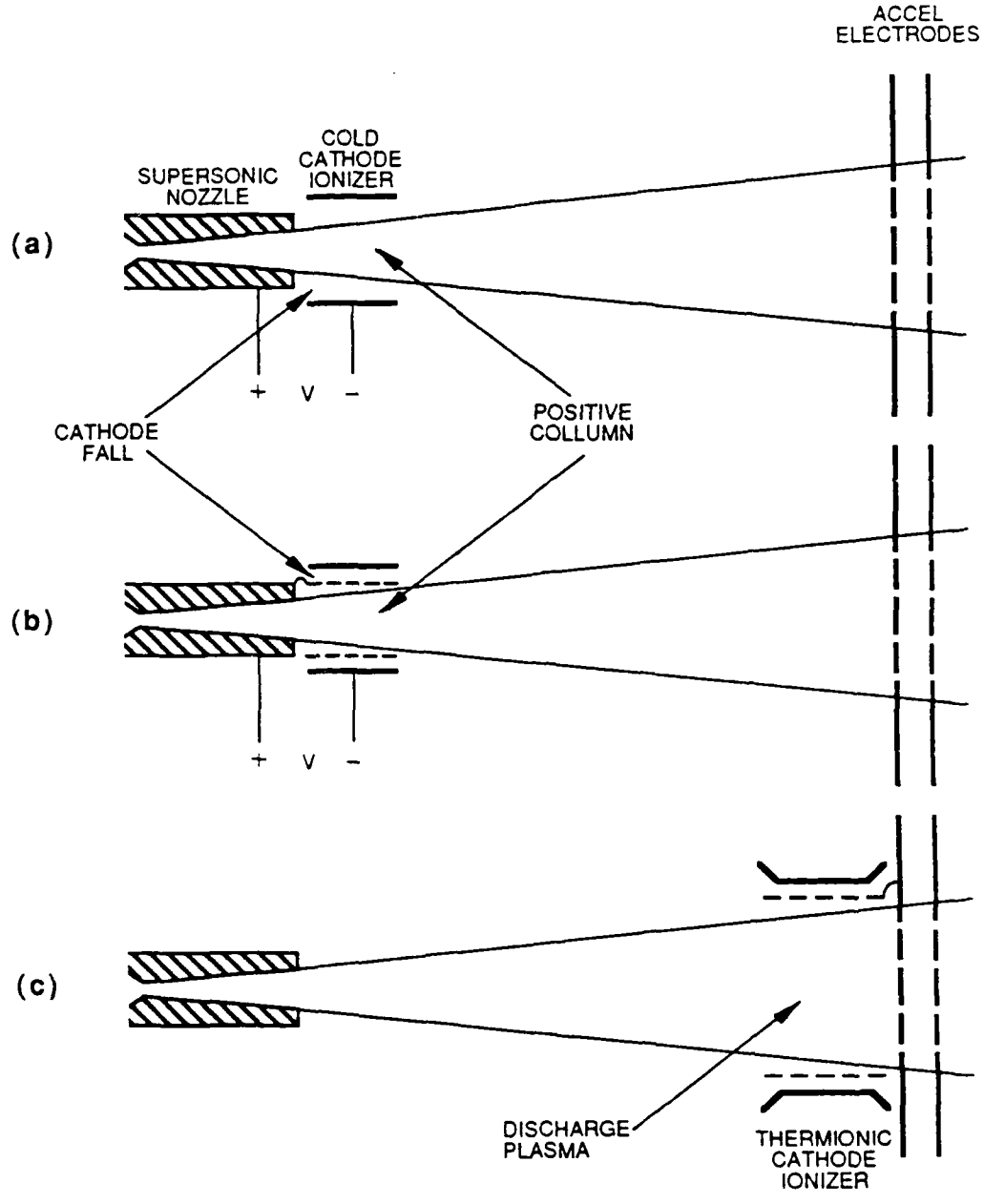

Figure 13. Ionizer configurations. (a) Basic (diode) cold cathode configuration whereby a cylinder is used as cathode and the nozzle serves as anode. (b) Modified (triode) cold cathode configuration with a mesh cylinder added as auxiliary anode. This anode serves to maintain a level of potential within the ionizing region. (c) Conventional thermionic ionizer.

support to this conclusion. It is noteworthy, however, that the retarding curve associated with the thermionic ionizer falls off more quickly than the two cold cathode ionizer curves. This suggests that fewer large clusters are ionized in the thermionic case, which may be attributable to the smaller electron energies. As far as the operational characteristics of cold cathode ionizers are concerned, the diode-type ionizer [Figure 14(a)] required a bias voltage of about 1 kV to generate electron currents close to 1 mA, where cluster ionization began to become saturated. These operating conditions were achieved with cathodes of beryllium/copper alloy, which has a high secondary emission coefficient. Unexpectedly, the triode ionizer [Figure 14(b)] required higher bias voltages (order of 4 kV) for the same emission currents. It is possible that the cathode cylinder chosen for this latter ionizer was too large for optimum performance.

The total cluster current produced by cold cathode ionizers was always smaller than that generated by thermionic ionizers, as shown in Figure 15. A possible reason for this difference is incomplete space charge neutralization within the drift region between ionizer and beam accelerator resulting in lateral beam spread beyond the geometrical beam boundaries.

3.2 CLUSTER BEAM DYNAMICS

3.2.1 Beam Extraction and Acceleration

Because cluster beam ionizers employ a discharge plasma as the ionizing agent, newly formed cluster ions must be extracted from this plasma with a suitable set of electrodes. Extraction can be accomplished with either a pair of single aperture plasma extraction and beam acceleration electrodes or, alternatively, with an equivalent pair of multiple aperture electrodes. Both methods are practiced with plasma-generated atomic ion beams. There, space charge forces often are large, and the inherent focusing action by the accel electrode pair is counteracted so

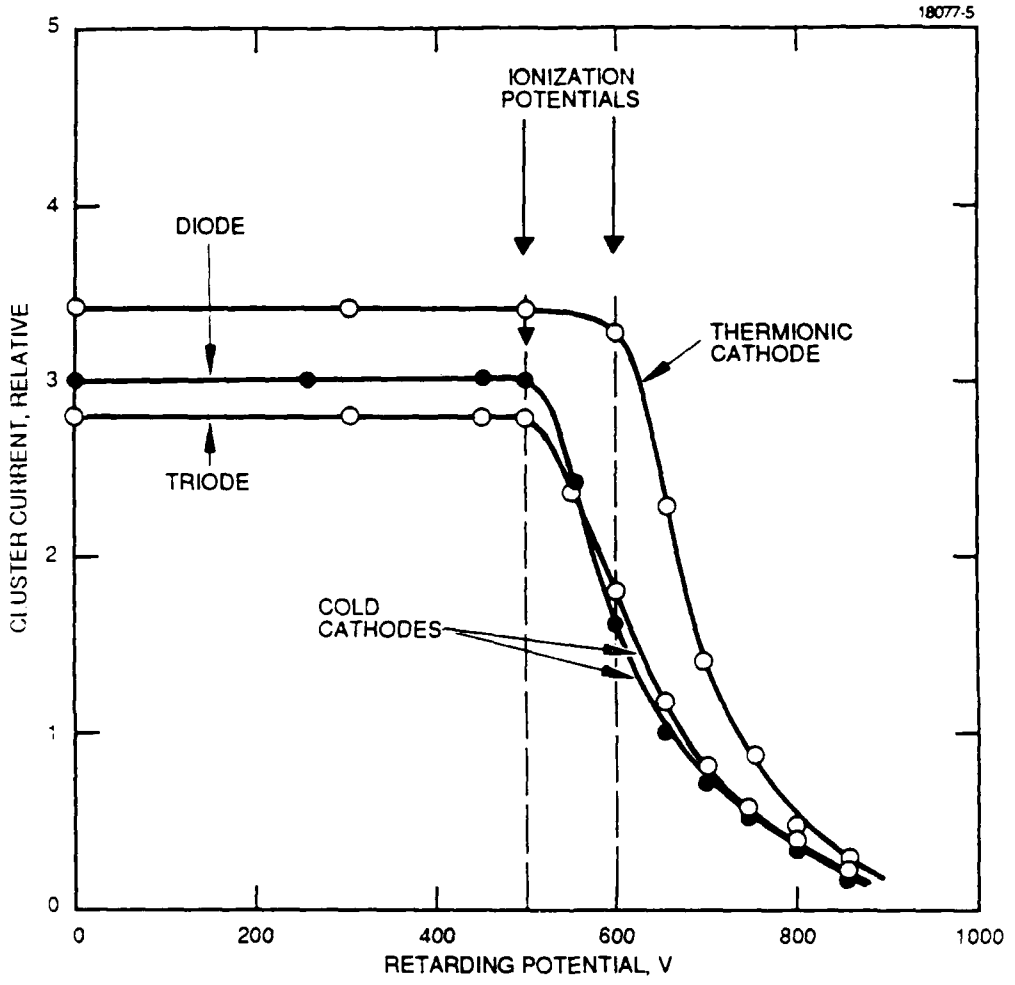

Figure 14. Retarding potential characteristics obtained with the ionizers shown in Figure 13. The purpose of this measurement is to determine whether the favored diode-type cold cathode ionizer generates ions within a narrow range of energies, as is required for mass separation. The similarity of the three retarding curves is considered evidence for a level-potential ionization process.

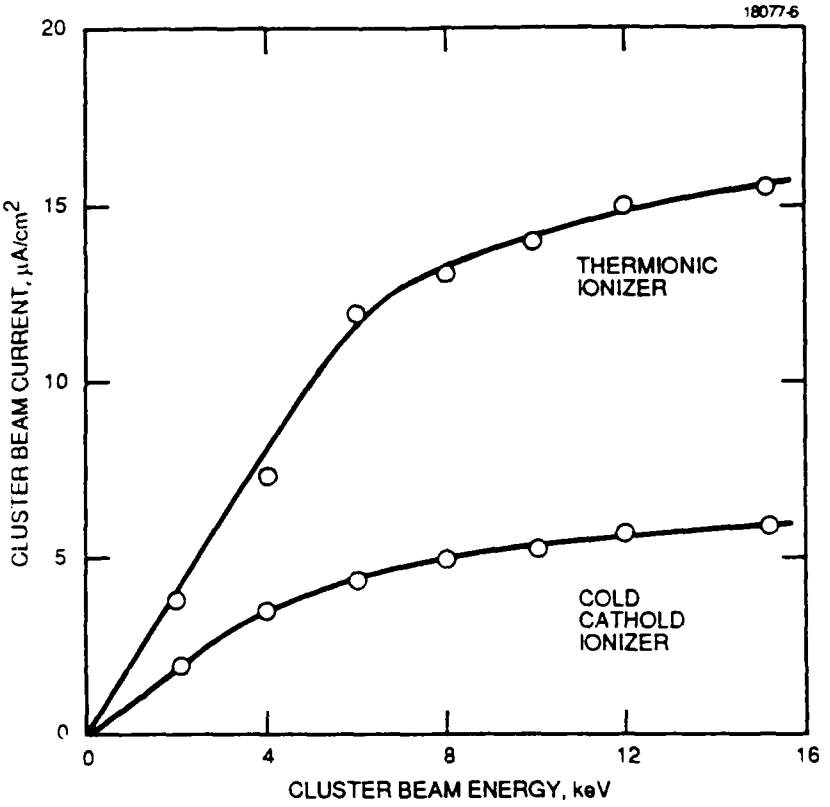

Figure 15. Argon cluster beam currents obtained with cold and thermionic cathode ionizers. The cold cathode ionizer results in lower current levels, probably due to a loss in ionized clusters along the drift region between ionizer and accelerator.

strongly that a beam focus does not form [see Figure 16(a)]. With cluster beams, space charge forces are much smaller and beam focuses (crossovers) are being generated [see Figure 16(b)]. Under these circumstances, multiple, small aperture extraction systems clearly are preferable because they result in a much less divergent beam. This superior collimation derives from the fact that, in first order, the focal length associated with an aperture pair is independent of aperture diameter. Hence, rays passing a pair of small apertures cross the focal point under smaller angles than rays from a set of large apertures [see Figures 16(c) and (d)].

A second advantage of multiple, small aperture beam extraction systems is that mass separation, which often is needed with cluster beam systems (see below), is best accomplished with a multiple, small aperture grid, spaced between extraction and accel electrodes. Mass separation requires a comparatively finely divided grid, because it relies on a uniform potential barrier across the cluster beam. If such a grid is incorporated, use of matching and aligned extraction and accel grids is a logical choice.

We have experimented with a number of beam extraction, mass separation, and beam acceleration electrode geometries. We have noted that, with axially extended ionizers where the plasma density is low, the mass separating grid can also serve as plasma extraction electrode, and only two electrodes are needed. With axially short ionizers, on the other hand, the plasma density is higher, and the plasma potential tends to ride up to the potential of the mass separator unless a third plasma boundary electrode is added. As far as the aperture size goes, diameters below 0.05 cm have been found satisfactory under our operating conditions. The spatial separation of the three electrodes does not appear to be critical. Typical separations between plasma extraction and mass separator electrodes were 0.2 cm, while those between mass separator and accel electrodes fell into the 0.5 to

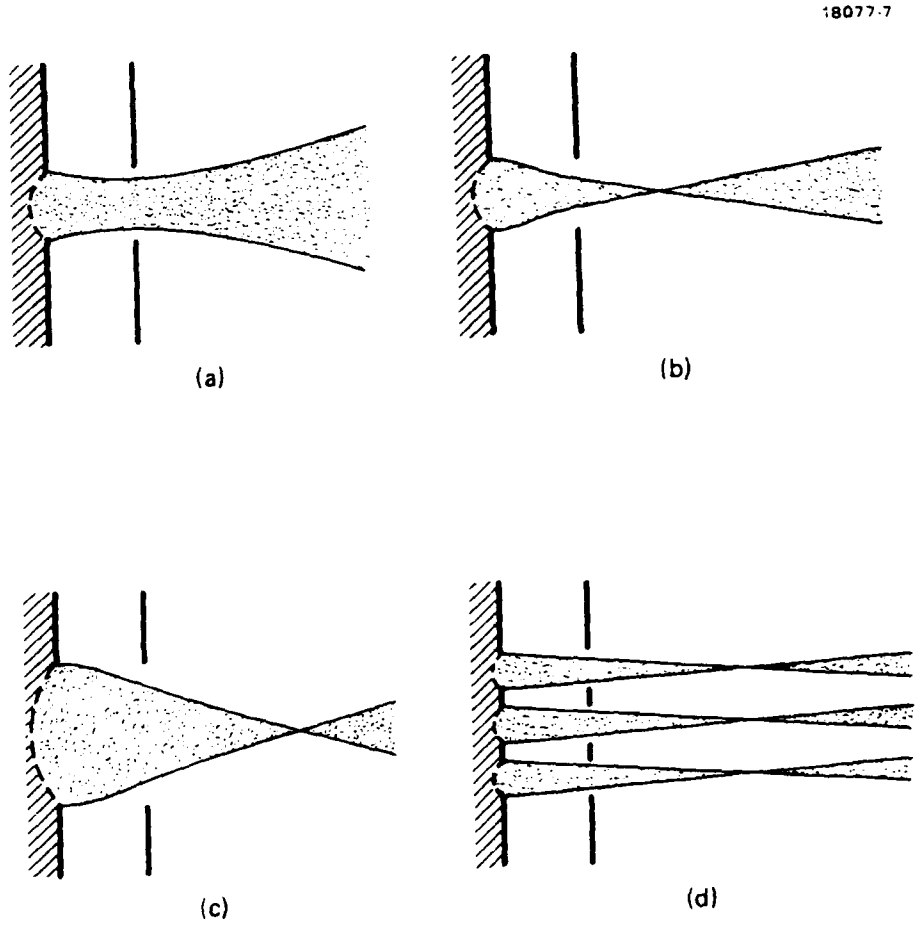

Figure 16. Ion beam extraction from a plasma ionizer. (a) Atomic ion beam formation, strongly affected by space charge forces. (b) Cluster beam formation, showing little space charge effect. (c) and (d) Comparison of single aperture versus multiaperture cluster beam extraction. Multiple beam is better collimated.

1.0 cm range. With such three-electrode beam forming systems, we have extracted cluster beams with current densities as high as 20 $\mu A/cm^2$ (at 70% grid transmission) and we have accelerated these beams to above 20 kV.

3.2.2 Cluster Mass Separation

Cluster beams derived from supersonic nozzles contain particles with a wide range of masses, including numerous individual atoms. If such beams are ionized and accelerated, particles with a similarly wide range of kinetic energies per atom are obtained. For example, if a mixture of singly charged clusters with 1000 atoms and atomic ions are accelerated through a 10 kV voltage difference, the clusters are energized to a level of 10 eV/atom, while the atomic ions reach 10,000 eV/atom. For film deposition applications, impact energies above about 50 eV/atom are undesirable, because particles with higher energies cause sputtering and lattice defects below the film surface. Accordingly, atomic ions and the smaller clusters cannot be tolerated in such applications.

We have developed a straightforward method for removing these low mass particles prior to beam acceleration. We have incorporated a small aperture grid as a retarding electrode between ionizer and beam accelerator (see Figure 8). The operation of this electrode is based on the experimentally confirmed expectation that particles of all masses exit the supersonic nozzle with very nearly the same velocity v_0. (In the nozzle, thermal kinetic and internal potential energy are converted into axial, directed kinetic energy; and an adequate number of collisions assures that clusters of all sizes reach the supersonic atomic beam velocity v_0.) As a consequence of this very narrow velocity distribution, the kinetic energy of clusters is proportional to their mass. A retarding grid, incorporated adjacent to the ionizer, thus is able to reject low mass particles. The mass limit m^* for rejection is related to the retarding potential V_{ret} by

$$m^{\wedge} = \frac{2eV_{ret}}{V_o^2} \quad .$$

For example, if argon clusters with up to 1000 atoms are to be eliminated from a beam with $v_o = 4 \times 10^4$ cm/s, a retarding potential of about 32 V must be applied.

Under this contract we have examined some of the important features associated with mass separating grids. The oscilloscope traces shown in Figure 17 provide a qualitative overview over the influence of a biased grid on the cluster beam. The top trace in Figure 17 was taken with a grid bias potential of approximately 50 V below the ionizer anode potential. In this situation, all ionized particles are passing through. The initial, short spike is generated by atomic ions produced by the shock wave in front of the supersonic gas pulse. The following ion current pulse, with a duration of about 1.5 ms (equal to the valve opening time) consists primarily of ionized clusters. The third, long-lasting pulse arrives after valve closure. This pulse decays very slowly, within a fraction of a second, and it consists solely of atomic ions (as determined by retarding probe measurements). These ions derive from a pressure build-up within and around the ionization cell after the supersonic gas stream has impacted on the ionizer structure.

The center and bottom traces in Figure 17 were obtained with the retarding grid at 10 and 60 V, respectively, above the ionizer anode potential. We can see that all atomic ions are removed from both traces. In addition, the cluster pulse height of the bottom trace is lower than that of the center trace, indicating that at the higher retarding potential clusters with less than about 1800 atoms have been eliminated.

A more quantitative assessment of low-mass cluster removal is possible on the basis of Figure 18, where Faraday cup retarding potential curves are shown for different mass separator grid potential levels. Each of the curves gives the energy

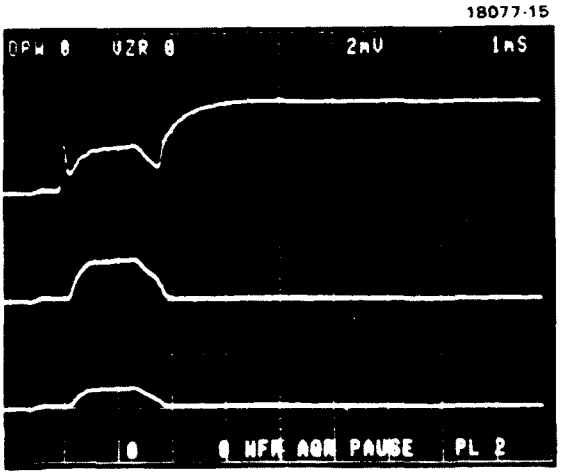

Figure 17. Cluster beam mass separation. The upper trace was obtained with the mass separation grid (see Figure 8) at a potential below that of the ionizer anode. The middle trace was taken with grid and anode at about the same potential. For the lower trace, the grid exceeded the anode potential by about 50 V.

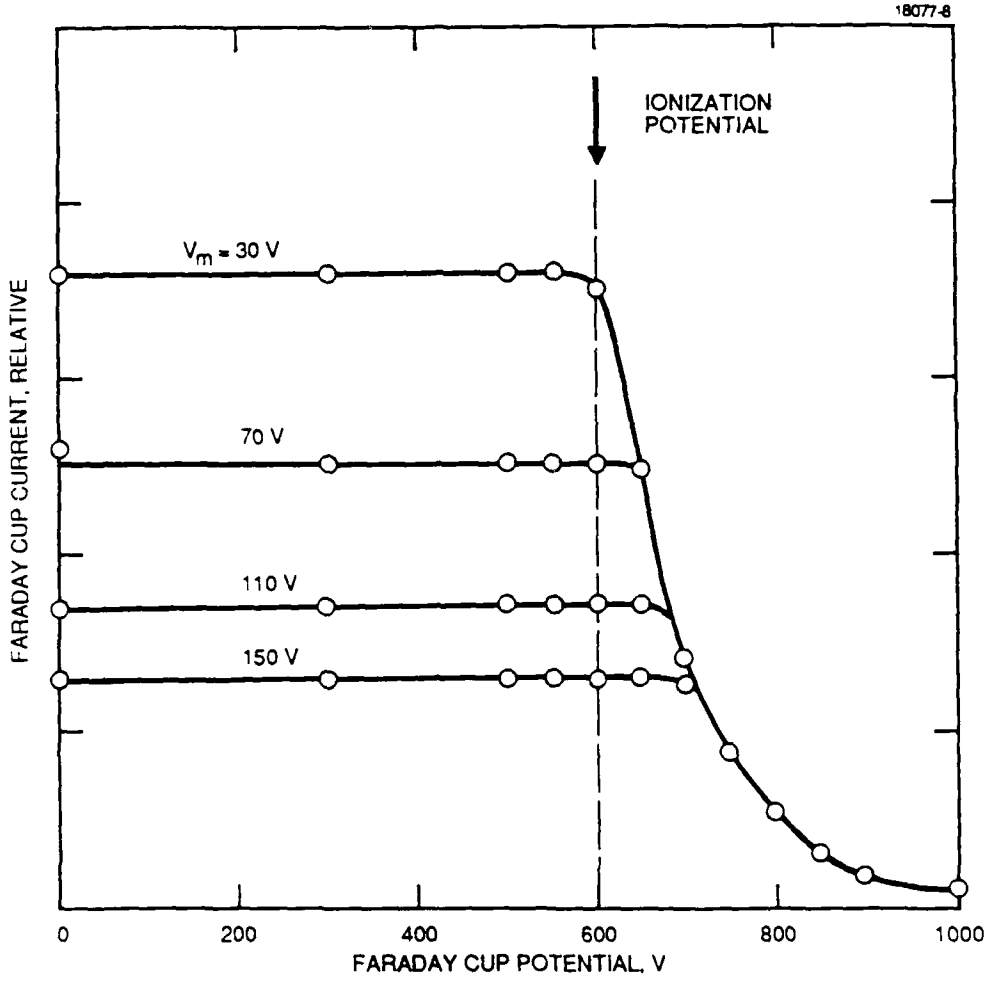

Figure 18. Cluster mass distributions measured after passage through the mass separation grid. As the grid potential is raised (from 30 to 150 V with respect to the ionizer anode), the mass cutoff potential increases from near zero to 100 V (see Figure 19).

(=mass) distribution of that beam portion passing through the mass separator grid and continuing to the Faraday cup. We can see that just as the mass separator grid potential is raised in steps, so is the cut-off level for small clusters.

It should be noted, however, that the mass cut-off steps are somewhat smaller than the mass separator grid potential steps. This deficiency is shown in Figure 19 and is attributable to the penetration of the accelerator electrode field into the mass separator grid openings. This field penetration lowers the average potential across the grid openings and, thereby, reduces the effective retarding potential. It is evident that the amount of field penetration varies with accelerator electrode potential. To illustrate this dependency, Figure 20 shows the measured changes in cut-off potential for atomic ions on applied acceleration voltage. As expected, this cut-off potential rises linearly with applied acceleration voltage. Based on these results, we conclude that mass separator grids can serve predictably and controllably to eliminate low-mass constituents from cluster beams.

3.2.3 Cluster Beam Transport

As we began to experiment with volatile cluster beams, we expected that, once a beam was ionized, mass-separated, and accelerated, transmission to a target would be a straightforward matter. We found, however, that drifting cluster beams undergo some changes. First, the current density decreases with distance, and second, beams lose energy with distance. Below, we describe our findings concerning these two phenomena.

3.2.3.1 Cluster Beam Space Charge Spreading. In examining the decrease in cluster current density with distance, we were quickly led to the conclusion that the cause of this decrease is lateral beam spreading resulting from space-charge forces. Because of the large mass-to-charge ratio of clusters, we had

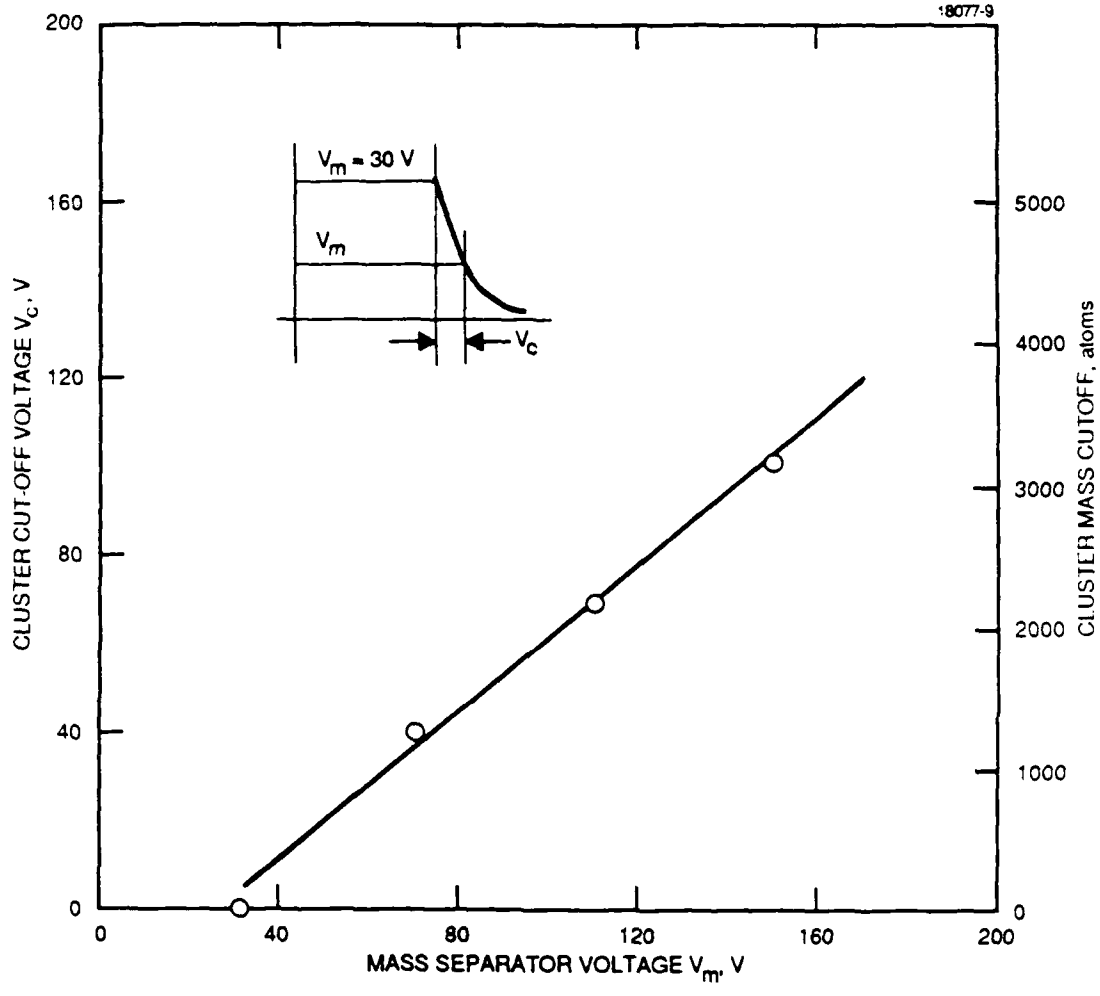

Figure 19. Low mass cluster cutoff characteristics, derived from Figure 18. Note that the slope of the curve is less than one, due to saddle points in the grid openings.

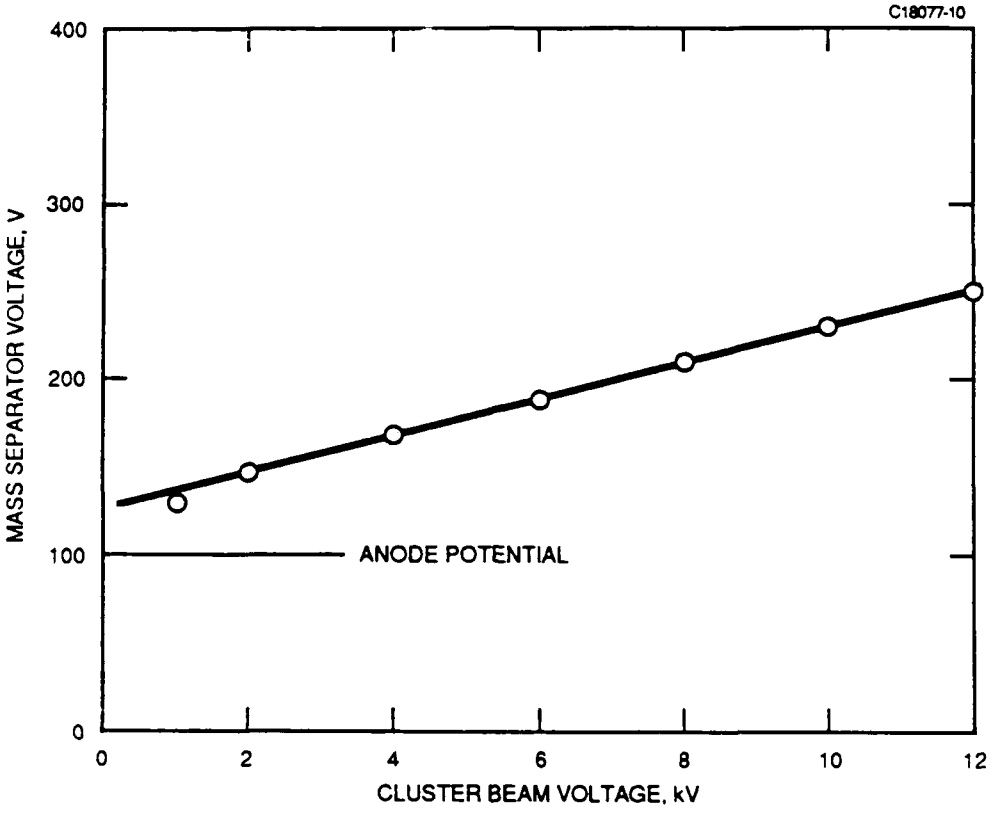

Figure 20. Effect of beam accel potential on mass separator grid effectiveness. As the accel potential is raised, higher grid potentials are needed to cut off atomic ions from the cluster beam. This dependence is due to the lowering of the saddle point potential in the grid openings with increasing accel potential.

assumed earlier that space-charge effects were negligible. The following assessment shows, however, that at acceleration voltages below about 10 kV, and for beam travel distances greater than about 10 cm, these forces are quite significant.

Lateral beam spreading from space charge was analyzed long ago in connection with the passage of electron beams through microwave tubes. The following expression, derived then, relates the beam radius r to the distance z that the beam has traveled

$$\int_1^r \frac{dr}{(\ln r)^{1/2}} = z\, K^{1/2}$$

$$\text{with } K = 4\pi \frac{j_o e}{m v_o^3} \quad ,$$

where j_o is the source current density (see Figure 21), and v_o is the beam velocity. Unfortunately, this relationship cannot be solved for r as a function of z, but tabulated values are available [Ref. 6]. We have converted and applied these electron beam data to the argon cluster beam with 1000-atom clusters, and have determined the target current density at a travel distance of 12 cm. Figure 21 shows the achievable target current density as a function of acceleration voltage and, parametrically, for different source current densities. Experimentally observed target current densities are also shown: these coincide well with the predicted current densities. The results given in Figure 21 support the conclusion that beam voltages in excess of 10 kV are required if space-charge spreading of cluster beams along drift lengths of some 10 cm or more is to be kept within acceptable limits.

3.2.3.2 Collisional Cluster Beam Interactions. During a series of mass distribution measurements, we observed that the cluster mass appears to depend on various beam parameters. We noted

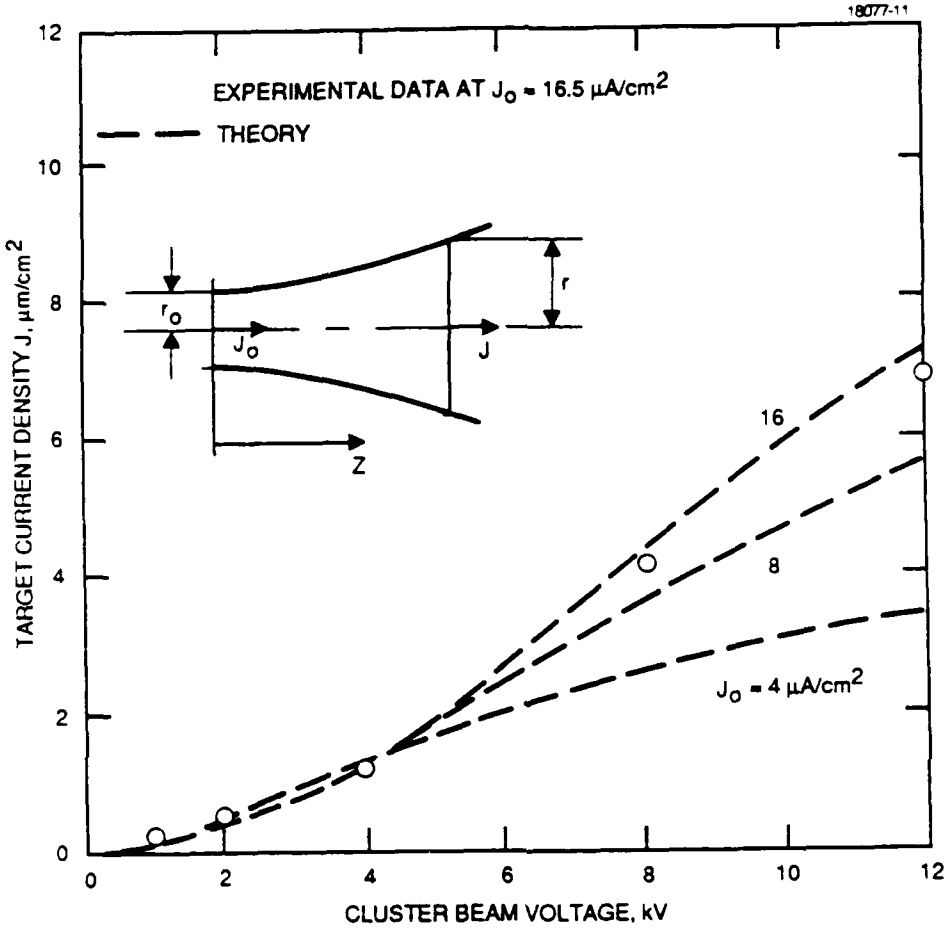

Figure 21. Theoretical (dashed lines) and experimental (circles) dependence of the achievable target current density T, at a distance of z = 12 cm from the accel electrode, as function of beam potential with the source current density T_o as parameter. The dependence found shows the restricting influence of space charge at low beam potentials.

dependencies on beam voltage (see Figure 22), on travel distance (see Figure 23), and on stagnation pressure (see Figure 24). Only the dependence on pressure was anticipated. Higher nozzle pressure is favorable for nucleation and growth and thus should lead to more, and to larger, clusters, as is evident in Figure 24. Not expected was the increased rounding with pressure of the retarding curve knee in Figure 24. Also not anticipated were any retarding curve variations either with beam voltage (Figure 22) or with drift distance (Figure 23.)

We examined these anomalies and found that they are attributable to collisions between ionized clusters and neutral gas atoms. As we have explained above, clusters and atoms leave the supersonic nozzle with near identical velocities. However, after ionization and acceleration, clusters begin to overtake the remaining neutral gas atoms. The resulting collisions can affect clusters in two ways. First, clusters can lose kinetic energy through momentum exchanges, and, second, clusters can lose mass by sputtering. According to the classical sputtering models, sputter erosion of such clusters is physically possible, because the impact energies (order of a few electron volts per atom) are well above four times the sublimation energy (about 0.1 eV). However, the rate of erosion should be extremely small. Measured sputtering rates for impact energies below 50 eV fall into the 10^{-6} to 10^{-3} range.

Based on these considerations, we conclude that the most likely cause for the observed curve changes is momentum (or energy) loss rather than mass loss. Below, a brief analysis of the anticipated momentum exchanges between clusters and gas atoms will be given.

In a situation where spherical clusters of i atoms, each with mass m, move with velocity v through a stationary gas cloud, collisions between clusters and gas atoms result in axial momentum losses of

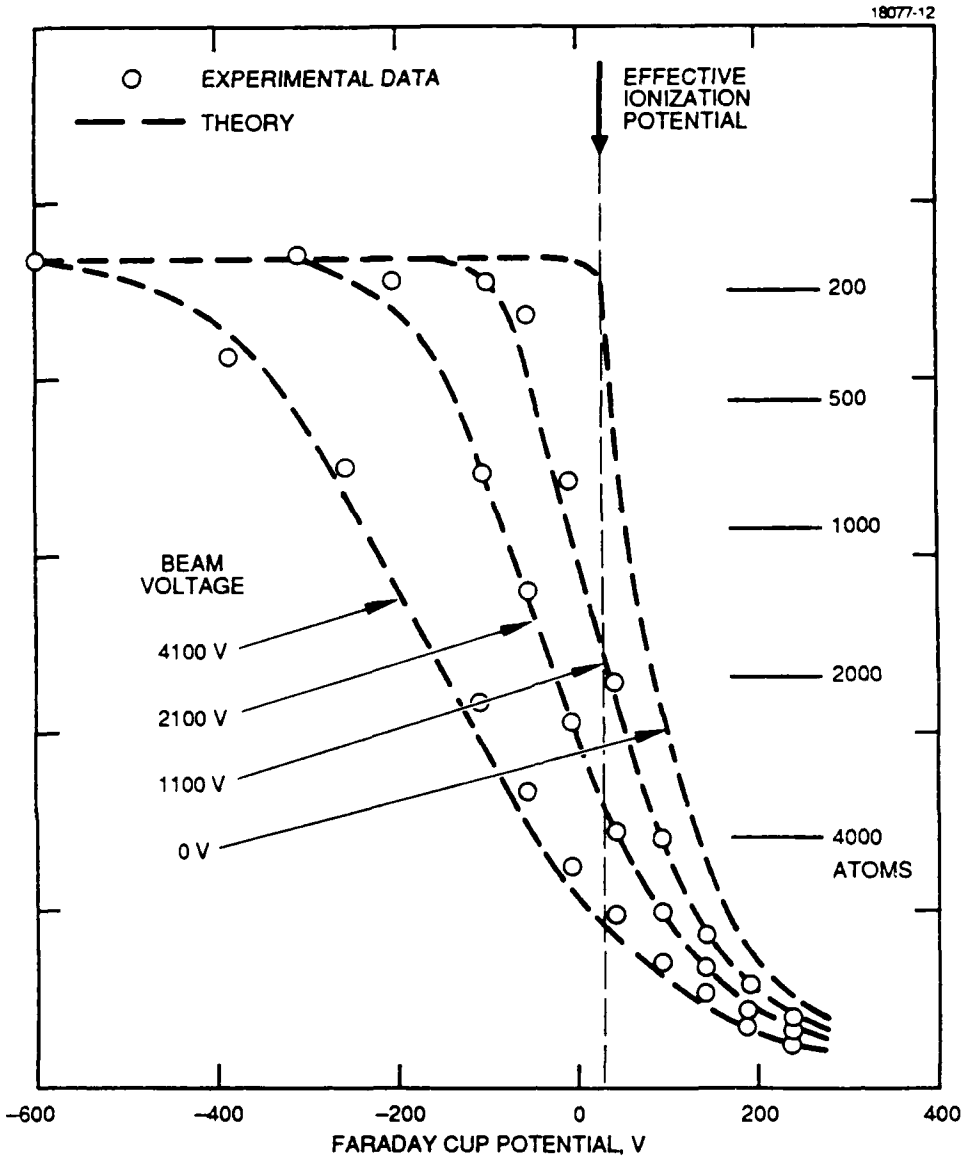

Figure 22. Observed and theoretically predicted changes in cluster beam energy distribution with beam acceleration potential. The circles represent measured data; the dashed lines are based on a theoretical model which assumes that the clusters are slowed down by collisions with neutral atoms in the supersonic gas stream.

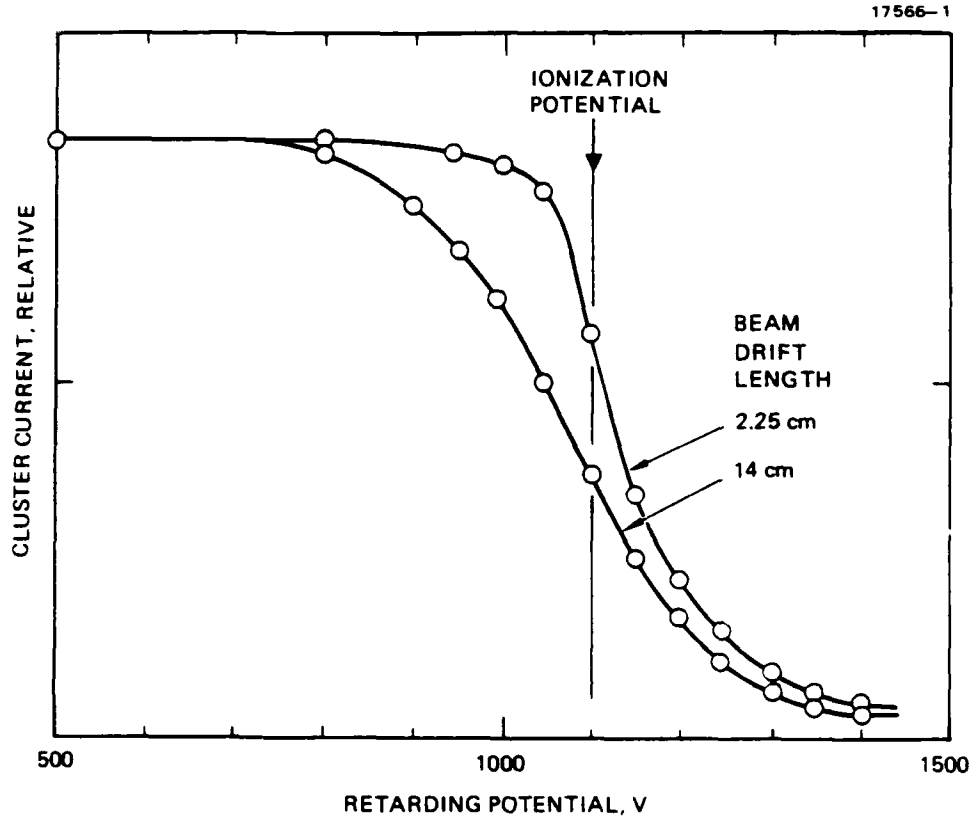

Figure 23. Observed changes in cluster beam energy distribution with different drift lengths of the beam.

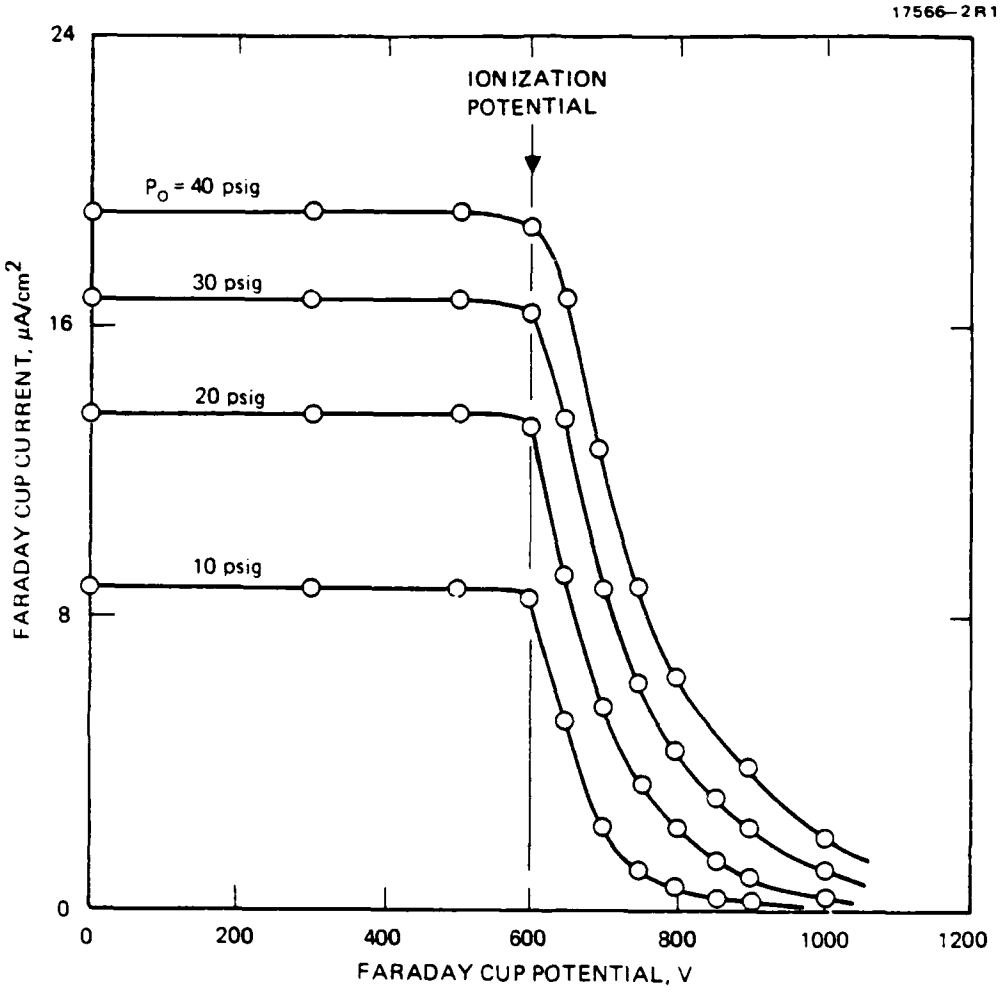

Figure 24. Observed dependence of the cluster energy and mass distribution with cluster source (= stagnation) pressure. The widening with pressure of the retarding curves is due to increases in cluster size, while the larger rounding near the ionization potential is attributed to collisional energy losses.

$$im\Delta v = 2\ mv\ (1-\sin^2\alpha) \quad ,$$

where α is the surface impact angle on the cluster. Averaging over all angles α on a spherical cluster reduces the momentum exchange to half the value at normal impact and leads to a cluster energy loss of

$$\delta E = mv^2 \quad .$$

The rate at which this energy loss occurs along a distance element dz is the product of δE with the number of atoms swept up by a cluster along a path of unit length

$$\frac{dE}{dz} = mv^2\ nA \quad .$$

Here, n is the volume density of gas atoms, A is the cross-sectional cluster area, given by

$$A = \pi \left(\frac{3i}{4\pi}\ V_a\right)^{2/3} \quad ,$$

and V_a is the volume of an atom in the cluster. Using these relationships, we can express the energy loss ΔE along a finite distance Δz as

$$\Delta E = \frac{1}{2} \left(\frac{36\pi}{i}\right)^{1/3} V_a^{2/3}\ nE_k\Delta z$$

whereby $$E_k = \frac{1}{2}\ imv^2$$

is the kinetic energy of the cluster. In terms of acceleration voltages V_{acc} and retarding potential changes ΔV, the last equation also can be expressed as

$$\Delta V = \frac{1}{2} \left(\frac{36\pi}{i}\right)^{1/3} V_a^{2/3} \, n \, V_{acc} \, \Delta z \quad .$$

In order to obtain numerical values for ΔV (which can be compared with measurements), V_a, n, Δz must be known. The atomic volume V_a can vary somewhat with cluster size and temperature. However, in the absence of specific information about these dependencies, we will use the atomic volume of condensed bulk material at the triple point. For argon at 84°K, V_a is approximately 4.7×10^{-23} cm^3. The gas density n in the interaction region can be determined from the following quantities: the rate of gas exhaust through the nozzle, the spreading angle of the gas exhaust, the flow velocity of the gas, and the distance from the nozzle. For the nozzle used (0.0125 cm diameter, 5° half aperture angle, and 2.4 cm length), for argon at room temperature and 20 psig, and for an (measured) exhaust velocity of 4×10^4 cm/s, the gas density in the interaction region (19 cm downstream of the nozzle mouth) was about 1.4×10^{14} atoms/cm^3. The length of the interaction region Δz was 2.25 cm.

These numerical values were entered into the above expression for ΔV. The resulting theoretical dependencies on cluster size i and beam voltage V_{acc} are shown in Figure 22 as dashed curves. As can be seen, theoretical and experimental dependencies agree well, confirming that energy losses of clusters along a drift region are primarily due to momentum exchanges and not to mass losses.

The question arises whether these losses interfere with ionized cluster beam applications in which surface reactions are to be energized. To estimate the energy losses in practical situations, we consider a beam drift length of 12 cm (instead of 2.25 cm) and a beam voltage of 20 kV (instead of 4.1 kV, as in Figure 22). According to the above expression for ΔV, energy losses should then be about 25 times larger than those shown in Figure 22. This increase leads to typical energy losses of about 5 keV out of 20 keV, which is considered very acceptable.

3.3 CLUSTER-ASSISTED DEPOSITIONS

The preceding sections described the work performed to develop the inert-gas cluster beam ionizer and acceleration system for reliably producing the cluster size and current required to match the average arrival rate of atoms in typical vapor deposition processes. This section discusses the investigation of cluster-assisted deposition conducted in the final year of this program.

3.3.1 Deposition Procedures and Objectives

As discussed earlier, the cluster-assisted deposition process uses the ionized cluster beam to energize the atoms during film deposition under the assumption that the kinetic energy of the cluster atoms can be transferred to the surface layer in the growing film. Conceptually, an increase in the atom energy should improve the mobility of the atoms, increasing the film density and promoting grain growth that will, in turn, improve film quality. To verify this concept, we selected cluster-assisted deposition of gold on GaAs as a process that could benefit from a low-temperature procedure, and a complete process sequence was developed for film growth. Procedures were developed for sample preparation, cluster beam setup, gold evaporation, and film evaluation. The objective was to determine the differences between films deposited by vacuum vapor deposition, and films deposited by ionized cluster-assisted vapor deposition, and the dependence on cluster beam parameters.

All the deposition experiments were carried out with the cluster beam apparatus configured as in Figure 25. The deposition substrate was held against its support with springs, and the temperature of the support was monitored with a thermocouple and could be controlled with a heater. For most deposition experiments, the substrate was not intentionally heated; however, the radiated heat from the vapor oven produced a substrate temperature increase of about 20°C. Figure 26 is a photograph of the substrate holder.

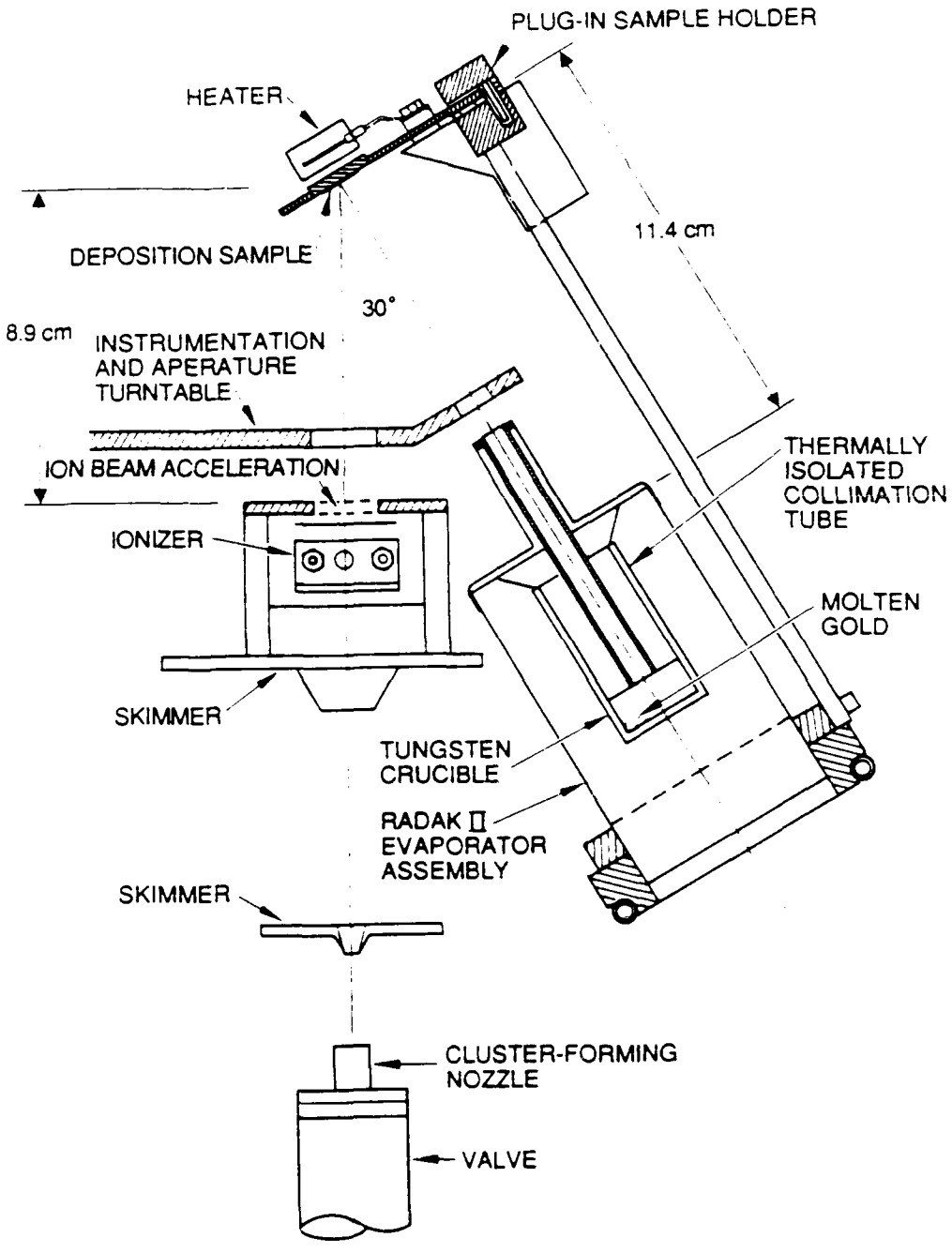

Figure 25. Experimental configuration for inert gas cluster-assisted deposition of gold on temperature controlled sample.

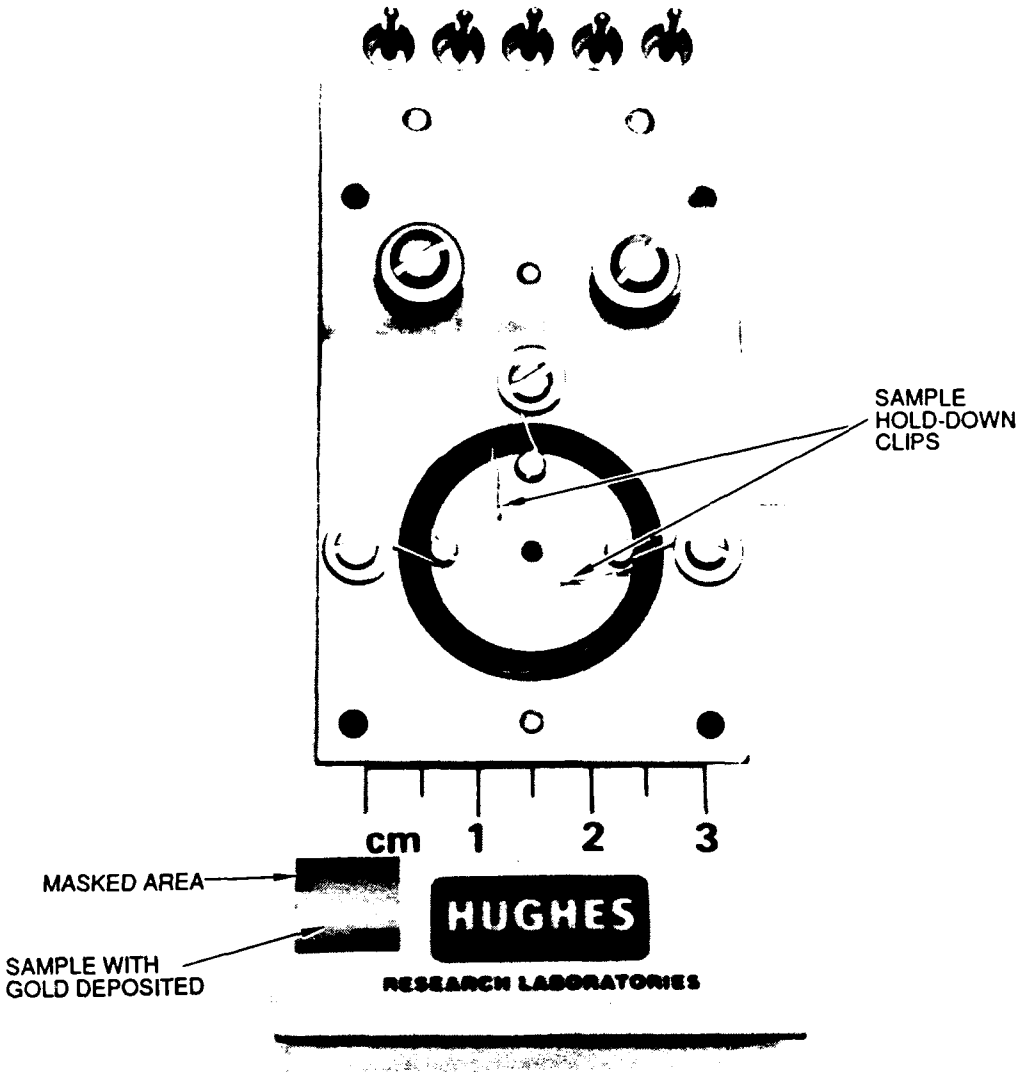

Figure 26. Photograph of sample holder and deposited sample. Springs hold sample against heated support and also maintain masking material in place (masked areas facilitate film thickness measurement).

The gold vapor source was a commercial radiation-heated crucible modified with a heat-shielded tube for better collimation of the vapor, and for prevention of direct line of sight between the substrate and the gold melt. The evaporator was operated to deposit films with a deposition rate in the 10 to 20 Å/s range. The vacuum enclosure was pumped by a liquid nitrogen trapped oil diffusion pump, and the base pressure was approximately 10^{-7} Torr.

The operation of the ionized cluster beam was described earlier; however, it should be noted here that cluster current is delivered in pulses, and for cluster-assisted deposition, the cluster beam operating conditions were adjusted so that the average arrival rate of cluster atoms at the substrate approximately matched the arrival rate of the depositing gold atoms. The arrival rate and average energy of the cluster atoms were varied as deposition parameters.

3.3.2 Deposition Results

Initial deposition experiments were carried out with minimum sample preparation under the supposition that cluster-assisted depositions would energize the substrate surface sufficiently to remove contaminants. The gold films deposited without substrate cleaning were of poor quality for both vacuum and cluster-assisted deposition. "Cleaning" the substrate surface by bombarding it with the ionized cluster beam produced no measurable improvement in film adhesion or appearance. Consequently, a wet chemical cleaning procedure was adopted for substrate preparation and, subsequently, all the deposited films were of relatively high quality. For GaAs substrates, this cleaning process consisted of ultrasonically agitated rinses in ocotron, acetone, methanol, propanol, deionized water, and dilute ammonium hydroxide, and a final rinse with deionized water. Samples were dried with filtered, dry nitrogen. At the outset, we thought there would be appreciable differences between the

properties of vacuum vapor deposited films and cluster-assisted vapor deposited films. This was not the case, however, and significant effort was therefore expended in refining the procedures for film deposition and for film analysis to find an explanation for the observed results. In all the depositions, the gold films displayed columnar growth with relatively fine grain structure. Columnar structures were on the order of 100 to 500 Å in diameter as seen in the microphotographs in Figure 27. Initially, we thought that the film morphology and grain structure could be correlated with cluster bombardment and the average energy of the cluster atoms. Subsequent experiments did not confirm this, however, and upon examining all the deposition data for gold on GaAs, we could not identify any significant effect on the film morphology that is attributable to the use of cluster-assisted deposition. We believe that the film morphology of the Au-GaAs system may be more dependent on the initial state of the surface nucleation sites than on the deposition conditions that can be appreciably changed by cluster beam bombardment.

The sheet resistance of the gold films was measured using a four-point probe instrument, and the resistivity of the films was found to be very low. The resistivity of most deposited samples was in the 4 to 6 $\mu\Omega$•cm range, which is comparable to values quoted in the literature for deposited and annealed thin gold films, and is about twice the resistivity value for bulk gold. Although the cluster-assisted deposition samples were typically slightly lower in resistivity than the vacuum-deposited films, the differences again were not very significant or consistent.

Cluster-assisted deposition was performed with xenon clusters so that Auger depth profiling could be used to determine whether cluster gas was incorporated in films deposited by the cluster-assist approach (the Hughes Auger system is set up to use argon ions for depth profiling; therefore, argon is always present). No xenon could be detected in the film (detection threshold is 0.1 at.%) and there was a sharp transition between

17271-1

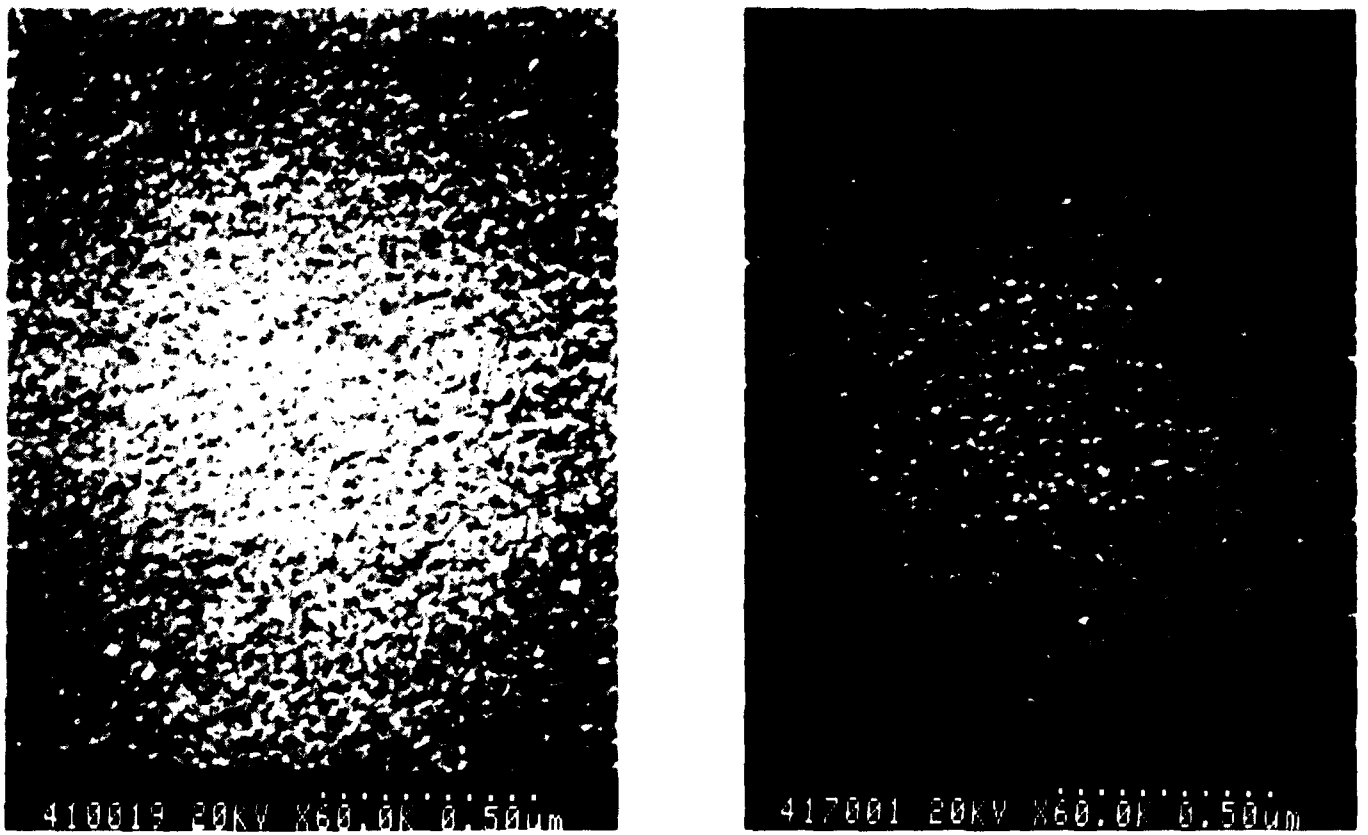

(a) VAPOR DEPOSITION

(b) CLUSTER–ASSISTED DEPOSITION

Figure 27. Microphotographs of gold film deposited on GaAs substrate by: (a) vacuum vapor deposition, and (b) cluster-assisted vapor deposition.

the film and the substrate (no interdiffusion of the gold or gallium). Also, it was evident that precleaning the substrate surface by bombardment with the low energy cluster beam did not remove the native oxide. Figure 28 shows a typical example of the depth profile measurements performed.

To summarize, cluster-assisted deposition was expected to improve the packing density and grain growth in films grown at low temperature. Because Takagi had observed appreciably improved film growth with low energy clusters, we performed the cluster-assisted depositions under this program using cluster energies in the 1 to 2 eV range, and with the substrate temperature near room temperature. Increasing cluster energy to 5 eV/atom and raising substrate temperature to 200°C did not improve film properties significantly. In searching for an explanation, it was found that analytical studies by Muller[7] of film deposition using clusters indicate that appreciably higher cluster energies may be required to cause impacting clusters to break up and transfer their energy to the depositing film. Moreover, other studies[8] using ionized vapor deposition (without clusters) have shown results similar to those reported by Takagi's laboratory. Consequently, the emphasis in the Hughes overall cluster studies program has returned to developing cluster sources capable of delivering a wider range of cluster energy (up to 20 eV/atom) and higher cluster flux (focused beams) for investigating the kinetics of cluster-surface interactions. Because the results reported by Takagi and his associates were probably achieved because of high energy ions (even though substrate damage is minimal), it has yet to be determined whether, and by what mechanism, ionized cluster impact improves film deposition or other surface reactions.

3.4 CONCLUSIONS AND RECOMMENDATIONS

When this program started, development of technology for producing ionized cluster beams for use in materials processing

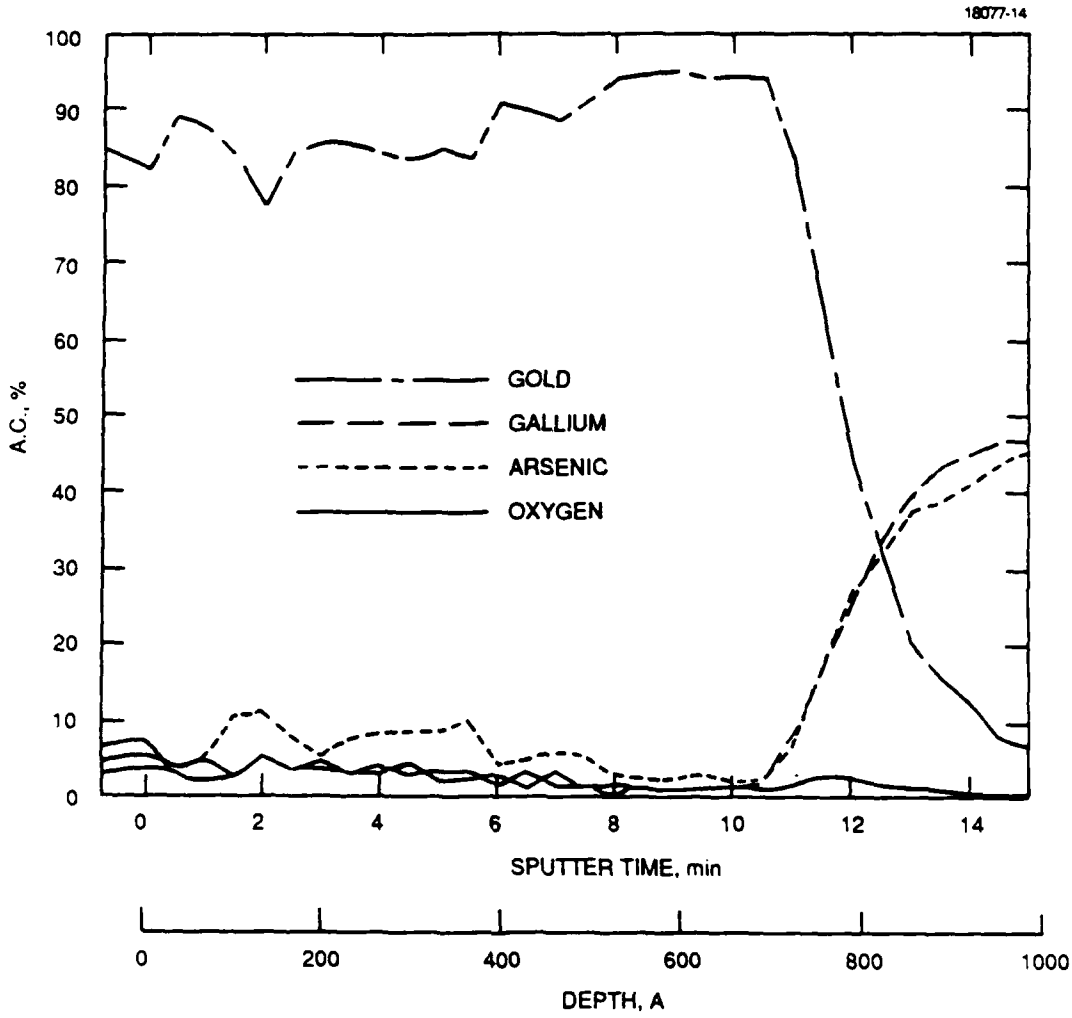

Figure 28. Depth profile of deposited film using Auger electron spectroscopy. Deposited film is ~700 Å thick with 200 Å transition. Native oxide not removed from substrate.

had just begun at the Hughes Research Laboratories. Most of the prior effort had been directed at establishing a basis for forming ionized cluster beams from nonvolatile materials in the fashion reported by Takagi. While the rate for cluster formation in these metal vapor sources cannot be shown to be viable for materials processing, the concept of using energetic cluster impact to control surface processes still appears attractive for process control. Significant progress has been made under this program in developing techniques for forming, ionizing, and accelerating inert-gas clusters for assisting surface processes. It was also shown that cluster energies have to be larger than a few electron volts per atom to appreciably affect cluster-assisted deposition. The details for achieving energy transfer to a surface process, and the requirements on ionized cluster beams for enhancing such surface processes, remain to be determined.

REFERENCES

1. T. Takagi, I. Yamada, and A. Sasaki, "Ionized-cluster beam deposition," J. Vac. Sci. Technol. 12, 1128 (1975).

2. W. Knauer, "Formation of large metal clusters by surface nucleation," J. Appl. Phys. 62, 841 (1987).

3. See also paper by W. Knauer and R.L. Poeschel, presented at 31st Intl. Symp. on Electron, Ion and Photon Beams, Woodland Hills, Calif., May 1987; to be published in J. Vac. Sci. Technol.

4. O.F. Hagena and W. Obert, "Cluster formation in expanding supersonic jets: effect of pressure, temperature, nozzle size and test gas," J. Chem. Phys. 56, 1793-1802 (1972).

5. H. Falter, O.F. Hagena, W. Henkes, and H.V. Wedel, Int. J. Mass Spectrom and Ion Phys. 4, 145 (1970).

5. W. Knauer, Final Report, Navy Contract N00014-86-C-0705, October 1987.

6. See, for example, K. Spangenberg, Vacuum Tubes (McGraw Hill, New York, 1948).

7. K.H. Muller, "Cluster-beam deposition of thin films: a molecular dynamics simulation," J. Appl. Phys. 61(7), 2516 (1 April 1987).

8. A. Choi, R. Ramanarayanan, S.N. Mei, and T.M. Lu, "Control of Al/Si(100) epitaxial orientations using a partially ionized beam," Paper presented at the 1987 spring meeting of the Materials Research Society, Materials Research Society, Anaheim, Calif., 21-25 April 1987.

APPENDIX

Ionised Cluster Beam Deposition

Ionized cluster beam deposition

W. Knauer and R. L. Poeschel
Hughes Research Laboratories, Malibu, California 90265

(Received 26 May 1987; accepted 4 September 1987)

An experimental cluster beam facility of the type used by Takagi was developed and tested. Since the cluster generation rate (of silver clusters in graphite crucibles) was small and not consistently observable, a basic study of the generation process was undertaken. Theoretical evaluation has revealed that clusters are formed on crucible internal surfaces and not in the vapor stream which passes out of the crucible through a nozzle, as had been assumed earlier. Experiments have confirmed this heterogeneous cluster growth model, showing that clusters occur consistently only when a temperature distribution is maintained within the crucible which favors cluster formation on surfaces near the crucible nozzle. A remaining problem is the low rate of cluster generation. This rate needs to be raised if metal clusters are to be used in practical film deposition apparatus. An alternative process which involves gaseous rather than metallic clusters is also under study. It is well known that isentropic expansion of gases, pressurized to a few atmospheres, results in homogeneous nucleation and can produce appreciable quantities of clusters with thousands of atoms. In order to utilize such gaseous clusters for film deposition applications, an assist mode is used in which films are grown by simultaneous vapor deposition and bombardment with energetic noble gas clusters. So far, a suitable cluster beam source has been developed, and deposition of gold films on GaAs substrates has been initiated, whereby ionized argon cluster beams provide the energy.

I. INTRODUCTION

In recent years various film growth processes have been developed which involve energetic particles to improve film quality. Some methods employ energetic neutrals (for example, sputter deposition); others rely on energetic ions of either the deposited species or of inert gases which serve as an assist to vapor deposition. The resulting films are generally denser, smoother, better adhering, and often of higher crystalline order than those obtained by vapor deposition. However, such films tend to contain point defects which are attributable to excessive impact energies of either all or some of the arriving particles.

T. Takagi *et al.*[1] have proposed and developed a low-energy film deposition method which, in principle, can avoid the formation of defects that occurs with beam processes. In this method, the material of interest is vaporized in a crucible and exhausted through a nozzle. Thereby, clusters of atoms are formed which, after ionization and acceleration, serve as carriers for growth material and energy to the film deposition site [see Fig. 1(a)]. If singly ionized clusters with hundreds of atoms are accelerated to voltages of a few kV, impact energies of tens of eV per cluster atom are obtained. Such energies are expected to provide the same beneficial film growth phenomena as occur in ion beam deposition, except that defect generation is avoided. In addition, large deposition rates are possible, since singly ionized, large clusters are little affected by space-charge forces.

In this paper, the results of a basic study of metal cluster formation will be presented and our experience with the Takagi process will be described. This discussion will show that, at present, generating clusters in metal vapors appears to be impractical for film deposition. An alternative use of clustered material for providing energy in deposition processes is being explored, and preliminary results will be presented. In this new approach, energetic noble gas clusters are used to assist vapor deposition [see Fig. 1(b)]. To distinguish the noble gas clusters of this later approach from the metal clusters of the Takagi process, we will use the labels "volatile" and "nonvolatile" for the two cluster species.

II. NONVOLATILE CLUSTER BEAM PROCESS

Our initial cluster beam tests were conducted with an experimental system of the type shown in Fig. 1(a). Using a graphite crucible, we vaporized silver and gold, exhausted the vapor through various nozzles, ionized and accelerated the efflux, and determined the mass distribution in the resulting beam under use of a retarding and also of a deflecting field analyzer. Both measurement methods showed that the nozzle efflux consisted primarily of single atoms. In some situations a small quantity of clusters with up to ~700 atoms was present. These clusters never constituted more than 1% of the total vapor efflux. Presence and absence of clusters was inexplicably connected with different types of heat shields, surrounding the nozzle section of the crucible. In order to understand this unexpected dependence, we conducted a theoretical and experimental investigation of metal cluster formation.

At first, we examined whether clusters could be generated by homogeneous nucleation (i.e., in the vapor phase), as proposed by Takagi. His predictions were based upon the well-established experience with gases, where supersonic expansion under sufficiently high pressure leads to homogeneous nucleation and to the growth of large clusters. Physically, the cluster formation process in gases is a result of isentropic cooling to temperatures where the level of supersaturation is so high that spontaneous condensation can occur.

To determine whether the vapor flow conditions in cruci-

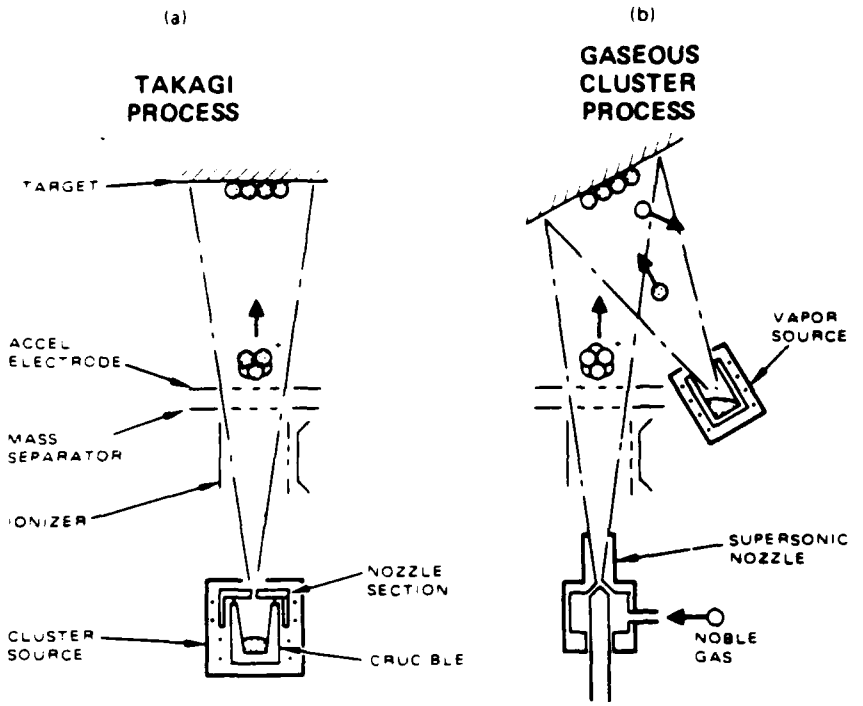

FIG. 1. Film deposition methods based upon ionized cluster beams: (a) process developed by Takagi, employing nonvolatile cluster materials for direct film deposition and (b) cluster-assisted film growth method, discussed in this paper, utilizing volatile noble gas clusters as an assist to vapor deposition.

ble nozzles are favorable for this type of cluster formation, we measured the vapor efflux from such nozzles. Using nozzle geometries (0.1-cm diameter, 0.1-cm length), materials (silver vapor and graphite crucibles), and pressure conditions (1–10 Torr) for which clusters had been seen previously,[1] we determined the quantity and angular distribution of the vapor efflux. The flow velocity was generally subsonic (Mach 0.4–0.6), as expected on the basis of estimated viscous effects within the thick boundary layer in the nozzle. Accordingly, the level of supersaturation in this situation is quite low and homogeneous nucleation will be a rare event. We also found the rate for growth of nuclei into large clusters to be extremely small. Such growth depends on collisions between vapor atoms and clusters on the way through the nozzle. Our analysis has revealed that only a small fraction of cluster-atom collisions results in atom attachment to clusters. The large majority of colliding atoms must leave again, since they serve to remove the heat of condensation associated with newly attached atoms. With metals, this removal process requires 10–100 extra collisions per attached atom. As a consequence, the vapor pressure in the crucible must exceed some 100 Torr, if clusters with hundreds of atoms are to be obtained. Since, experimentally, cluster growth to this size range was observed already at pressures below 10 Torr, this growth must be attributed to a different process.

The logical alternative to volume growth is cluster formation on surfaces, i.e., heterogeneous nucleation and growth. To determine the relevance of this hypothetical process, we have analyzed the following growth aspects: (1) formation of metal vapor nuclei on internal crucible surfaces; (2) growth of surface nuclei into larger clusters, and (3) ejection of clusters from crucible surfaces. The details of this analysis are described elsewhere.[2] Results obtained can be summarized as follows: For many metal vapors in contact with typical high-temperature crucibles, surface nucleation occurs at very high rates. For example, with silver vapor of ~1-Torr pressure, the nucleation rate on a graphite surface reaches 10^{18} nuclei/cm^2 s. Cluster growth beyond the nucleus state occurs rapidly, too, (order of 10^4 atoms/s and is determined by the difference between atom arrival and reevaporation rates. The arrival rate at the cluster site is determined by the saturated vapor pressure and, therefore, by the temperature T_1 of lower crucible section, where the metal is evaporated. The rate of reevaporation from a cluster is given by the temperature of the cluster growth surface, i.e., by the temperature T_2 of the upper crucible section, near the nozzle. If T_2 is significantly lower than T_1 ($\Delta T \sim 50$ °C with silver on graphite) cluster growth is very vigorous and continues to the macroscopic droplet state. If T_2 is close to T_1 ($\Delta T < \sim 30$ °C), growth eventually comes to a standstill and clusters of a finite size are obtained. If T_2 is about equal to or larger than T_1, no growth occurs and the surface remains crowded with atoms and nuclei.

As far as cluster ejection from the growth surface is concerned, the two decisive factors are adhesion force and surface temperature. Some metals (primarily those of groups IB, IIB, IIIA, IVA, VA, and VIA in periods 4, 5, and 6 of the periodic system of elements) do not wet graphite and other high-temperature crucible materials and, therefore, are attached with low adhesion energies in the 150–300 erg/cm^2 range. In these cases, entire clusters with a few hundred atoms (of which only a few dozens are forming the interface surface) are attached with a few eV only. At the high temperatures at which crucibles are operated (~1600 K with

silver), such clusters are ejected rapidly (at rates on the order of 10^{12} to 10^{13} atoms/cm^2 s for silver on graphite). However, with rising cluster size, the surface dwell time increases rapidly, and larger clusters with more than a few hundred atoms remain on the surface sufficiently long to overcrowd or "clog" the surface. As a result, many of these larger clusters coalesce into still larger clusters and even microdroplets, with much longer surface dwell times. In the case of silver clusters on graphite, surface clogging is expected to occur when the cluster size exceeds ~700 atoms.

To test this surface generation model, several types of crucibles and associated electron-bombardment heating configurations, in which the temperatures of the upper and lower crucible sections could be controlled separately, were built and evaluated. The tests consisted in measurements of the angular distribution of the nozzle efflux. It had been observed earlier that, in the presence of clusters, the angular flow distribution shows a central hump, indicating that clusters are more collimated than individual atoms. This collimation is to be expected, since clusters (which move through the nozzle with the same speed as atoms) possess much smaller random velocities, due to their higher mass. Figures 2(a) and 2(b) show measured silver vapor flow profiles.

In Fig. 2(a) the temperature of the upper crucible section is maintained significantly above that of the lower crucible section, and the efflux contains no clusters. In Fig. 2(b) the upper crucible temperature is kept nearer that of the lower section, and here clusters are observed. From the width of the hump, an average cluster mass of 500 atoms can be inferred, while the hump height indicates a maximum flux of about 10^{12} clusters/s, or a fraction of about 0.5% of the total vapor efflux.

Practical experience has shown that the ionization efficiency of such clusters is limited to a few percent. Therefore, deposition rates in the range of 10^{-2} to 10^{-1} Å/s can be expected. Since these rates are considered marginal for practical use, further improvements in cluster generation efficiency are considered essential.

III. VOLATILE CLUSTER BEAM PROCESSES

As discussed above, clusters can be formed by homogeneous nucleation when a gas is expanded isentropically through a supersonic nozzle from relatively high pressure into vacuum. Extensive studies of this type of cluster formation process have been conducted by others (see review paper by Hagena[3]). Our efforts have concentrated on the generation of large clusters (> 1000 atoms), the formation of collimated ionized cluster beams, and the deposition of films under ionized cluster assistance.

The experimental configuration for cluster formation, ionization, and beam extraction is shown schematically in Fig. 3. The cluster beam apparatus is operated on a pulsed basis (1%–5% duty cycle) to ease the pumping requirements. For a given nozzle geometry and temperature, the average cluster size is determined by the reservoir pressure. Ionization is achieved by electron bombardment with currents of a few mA and with energies in the 80–100 eV range. An ion beam is extracted and accelerated through grids with aligned apertures. Cluster current and size distribution are measured by collecting the ion beam in a Faraday cup equipped with a grid. By applying a retarding potential to the grid, energy distributions like that shown in Fig. 4(a) are obtained. Atoms and clusters of all sizes are expected to possess the same, maximum expansion velocity v_s given by

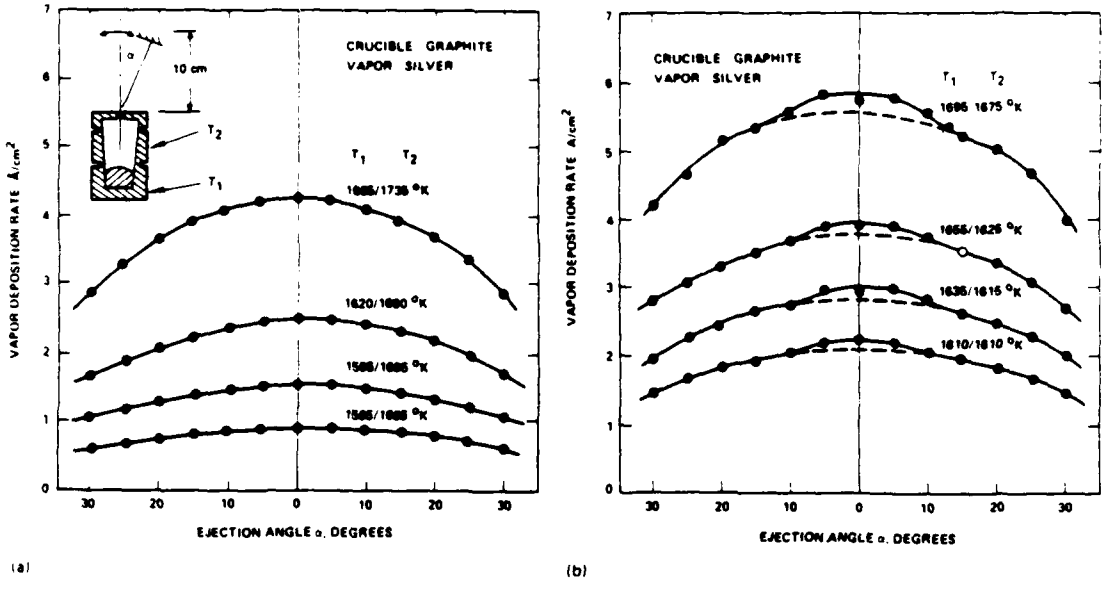

FIG. 2. Measurement of the angular distribution of the vapor efflux from a crucible nozzle: (a) upper crucible body at a temperature somewhat above that of the lower body and (b) upper and lower crucible temperature close to each other. In this situation, cluster growth on inner crucible surfaces is favored. The central lump is considered evidence for such clusters.

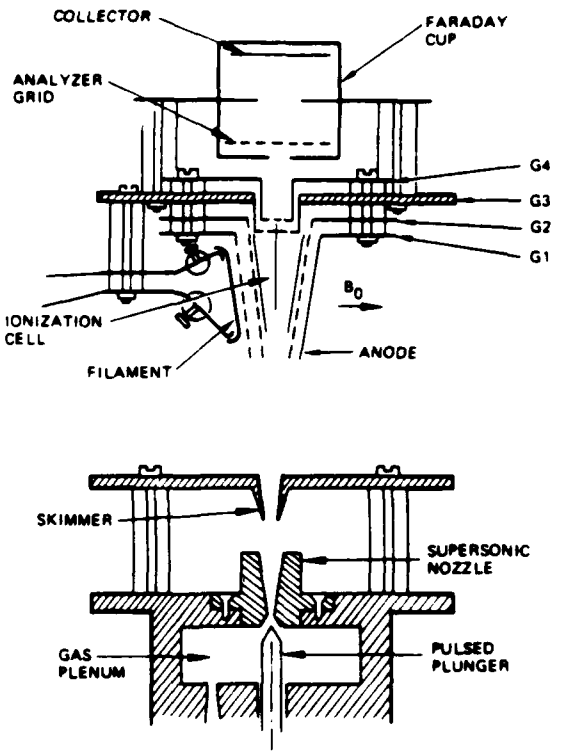

FIG. 3. Experimental configuration of nozzle, skimmer, ionization cell, and detector for investigation of cluster generation in inert gases.

$$v_s = \sqrt{(2\gamma/\gamma - 1)(kT/m_0)},$$

where γ is the ratio of specific heats, T is the nozzle temperature, k is Boltzmann's constant, and m_0 is the mass of the gas atom. Accordingly, the energy scale in Fig. 4(a) can be converted into a cluster size scale by the relationship:

$$N_a = (2\ \text{eV}/m_0 v_i^2),$$

where N_a is the number of atoms of mass m_0 in a cluster, and v is the retarding voltage (with respect to the potential of the ionizer anode).

Much of our initial effort has been devoted to experiments which served to reproduce the results described by Hagena and Obert[4] with regard to cluster-size dependence on reservoir pressure on gas type, and on nozzle dimensions. It was also necessary to optimize the ionization cell and beam forming elements to obtain useful quantities of ionized clusters. The eventual objective of our gas cluster study is to determine whether inert-gas ionized cluster beams can be used to impart energy to surface processes such as thin-film deposition or epitaxy. As with the Takagi process, it should be possible, in principle, to inject energy into these processes on an atomic basis, without causing the dislocation damage observed in high-energy ion beam processes. To avoid any damage with cluster beams, all atomic ions must be removed from the beam, since atomic ions reach excessive levels of

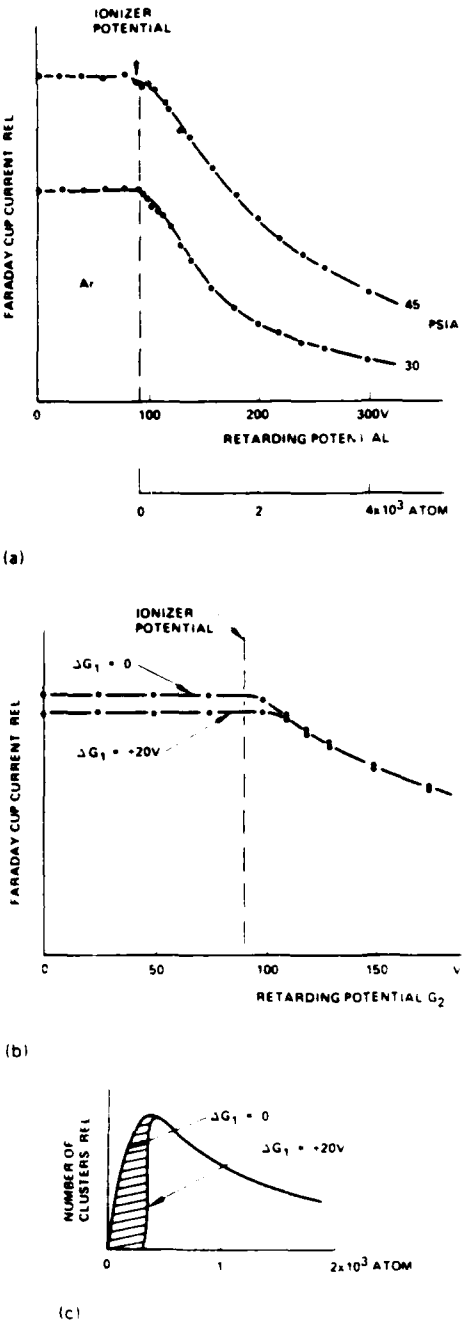

FIG. 4. Representative curves obtained with the gridded Faraday-cup probe showing collector current retarding potential for several ionization cell operating conditions: (a) typical data obtained for determining cluster size distribution (note that retarding potential scale can be calibrated in number of atoms per cluster); (b) typical data obtained by variations in mass separator grid bias (returns atomic ions and small clusters to ionization cell interior); and (c) distribution of cluster size derived from data in (b), illustrating electrostatic mass separation

kinetic energy when accelerated by the extraction grid system. As shown in Fig. 3, atomic and small cluster ions can be prevented from entering the ion beam by applying a bias voltage to grid 3 such that this grid is maintained a few volts

positive with respect to the ionization cell anode potential. Figure 4(b) shows retarding potential characteristics for two different grid bias conditions. If these characteristics are compared, as shown in Fig. 4(c), the electrostatic elimination of atomic and small cluster ions becomes evident. Clearly, it is possible to specify the smallest cluster size that will be accelerated in the ion beam by adjustment of this grid voltage in the cluster beam apparatus shown in Fig. 3.

We have only begun to study the effects of volatile, ionized, and energized clusters in film deposition processes. Our initial experiments are being carried out on the type of cluster-assisted vapor deposition system shown in Fig. 1(b). In order that we may realize the potential benefits of energetic particle impact, we have established the following guidelines for the depositions:

1. The cluster energy should fall into the range of 1 to 10 eV per atom, which is well below the damage threshold. With clusters of about 2000 atoms (which are convenient to generate), this implies acceleration voltages between 2 and 20 kV.

2. The rate of delivery of energetic clusters should be related to the film deposition rate such that, on average, a dose of at least 1 eV is available for each arriving film atom. At a deposition rate of 10 Å/s this condition implies an impact rate of about 10 μA/cm^2 with clusters of 2000 atoms, accelerated to 5 kV, and pulsed with a duty cycle of 2%.

So far, we have deposited gold films on GaAs substrates under assist from argon clusters. The rate of deposition, cluster arrival, and kinetic energy delivery were maintained approximately at the above stated levels. The deposited films have excellent appearance and adherence, but a detailed analysis of the film morphology has not been completed at this time. Sheet resistance measurements showed only insignificant differences in comparison to vacuum vapor-deposited films. We speculate that to achieve significant improvements over vapor-deposited films, the kinetic energy of the cluster ions will have to be increased, and we are presently seeking to raise the cluster kinetic energy from ~2–3 eV/atom to levels close to 10 eV/atom.

IV. CONCLUSIONS

Theoretical, as well as experimental, evidence provided in this paper suggests that metal clusters, formed in hot crucibles, result from surface rather than volume condensation. According to the theory, clusters should form only when a unique temperature gradient is maintained along interior crucible walls. This dependence was confirmed experimentally; however, even with the most favorable temperature gradients, only ~1%–2% of the vapor efflux became condensed into clusters. We believe, therefore, that earlier film depositions under use of crucible-type cluster sources have involved insignificant numbers of clusters, if any. Rather, the energizing constituents in these depositions likely were atomic ions with several keV energy per atom.

Unlike the crucible method, our own approach to cluster deposition, which involves noble gas clusters as an energizing assist to conventional vapor deposition, provides ample numbers of clusters with energies in the range 1–20 eV atom. We monitor these clusters before each deposition with a retarding field probe and we remove all atomic ions and small cluster ions. Thus, we believe to have under study the first truly cluster-based deposition process. Our initial depositions with 1–3 eV atom clusters showed limited beneficial effects and much more needs to be done to determine whether, how, and to what degree clusters can improve film growth.

ACKNOWLEDGMENTS

This paper was supported in part by ONR, Contract No. N00014-86-C-0705, and by AFOSR Contract No. F49620-85-C-0125.

[1] T. Takagi, I. Yamada, and A. Sasaki, J. Vac. Sci. Technol. 12, 1128 (1975).
[2] W. Knauer, J. Appl. Phys. 62, 841 (1987).
[3] O. F. Hagena, in *Molecular Beams and Low Density Gas Dynamics*, edited by P. P. Wegener (Dekker, New York, 1974), pp. 93–181.
[4] O. F. Hagena and W. Obert, J. Chem. Phys. 56, 1793 (1972).